PARAMETRIC STUDY OF DIAMOND WHEEL DICING PROCESS IMPROVEMENT

KATCHAMART MANOKRUANG

A THESIS SUBMITTED IN PARTIAL FULFILLMENT
OF THE REQUIREMENT FOR THE DEGREE OF
MASTER OF ENGINEERING IN COLLEGE OF DATA STORAGE TECHNOLOGY
INTERNATIONAL COLLEGE
KING MONGKUT'S INSTITUTE OF TECHNOLOGY LADKRABANG
2014

KMITL-2014-IC-M-005-006

PARAMETRIC STUDY OF DIAMOND WHEEL

DICING PROCESS IMPROVEMENT

KATCHAMART MANOKRUANG

A THESIS SUBMITTED IN A PARTIAL FULFILLMENT
OF THE REQUIREMENT FOR THE DEGREE OF
MASTER OF ENGINEERING IN COLLEGE OF DATA STORAGE TECHNOLOGY
INTERNATIONAL COLLEDGE
KING MONGKUT'S INSTITUTE OF TECHNOLOGY LADKRABANG
2014
KMITL-2014-IC-M-005-006

หัวข้อวิทยานิพนธ์	การศึกษาพารามิเตอร์ของการตัดเพื่อเพิ่มประสิทธิภาพของใบตัดกากเพชร
ชื่อนักศึกษา	นายคัชมาตร์ มะโนเครื่อง
รหัสประจำตัว	53600601
ปริญญา	วิศวกรรมศาสตรมหาบัณฑิต
สาขาวิชา	เทคโนโลยีบันทึกข้อมูล
พ.ศ.	2557
อาจารย์ผู้ควบคุมวิทยานิพนธ์	ผศ.ดร.มนต์ศักดิ์ พิมสาร

บทคัดย่อ

อุตสาหกรรมผลิตฮาร์ดดิสก์ไดรฟ์ (HDD) เป็นอุตสาหกรรมที่มีการแข่งขันสูง การพยายามลดต้นทุนการผลิตจะเพิ่มความสามารถในการแข่งขันของอุตสาหกรรม ในงานวิจัยนี้ให้ความสนใจในส่วนวิธีการลดต้นทุนการผลิต จากการเพิ่มอายุใบตัดกากเพชร โดยลดการสึกหรอ ในกระบวนการตัดหัวอ่านฮาร์ดดิสก์ไดรฟ์แยกออกจากกันและยังคงคุณภาพคือขนาดรอยกะเทาะของขอบตัดและความหยาบของผิวตัด

การศึกษาถึงผลกระทบของ มุมหัวฉีดน้ำหล่อเย็นและอัตราการไหล ที่มีผลต่อการสึกหรอของใบตัดกากเพชร ขนาดของรอยกะเทาะและความหยาบของผิว โดยใช้หลักการของการออกแบบการทดลอง (Design of experiment, DOE) สร้างสมการความสัมพันธ์ ด้วยหลักการของวิธีผลตอบสนองพื้นผิว (Response surface method, RSM) และ หาจุดที่เหมาะสมด้วยวิธีการอ๊อพติไมเซชั่น

ผลจากการวิเคราะห์พบว่า มุมหัวฉีดที่ 19.7° และอัตราการไหลของน้ำหล่อเย็นที่ 3.2 แกลลอนต่อนาที ให้ผลที่ดีที่สุด และเมื่อนำไปทดลองใช้จริง สามารถลดการสึกหรอและเพิ่มอายุการใช้งานใบมีดได้ถึง 25%

คำสำคัญ: การตัดชิ้นงานด้วยใบตัดกากเพชร พริซิชั่นไกรน์ดิ่ง ฮาร์ดดิสไดร์ฟ สไลเดอร์บาร์

Thesis title:	Parametric Study of Diamond Wheel Dicing Process Improvement
Student:	Mr. Katchamart Manokruang
Student ID:	53600601
Degree:	Master degree of engineering
Program:	Data storage technology and applications
Year:	2014
Thesis advisor:	Asst. Prof. Dr. Monsak Pimsarn

ABSTRACT

The Hard Disk Drive (HDD) industry is highly competitive. Cost reduction in manufacturing is a very important to remain competitive. This research focuses on to extend the life of the diamond blade by reducing the wear rate in head part cut off process. This will help to reduce one of the costs of slider production, the frequency of replacing the worn-out diamond wheel. In addition to extending the life of the diamond wheel, the process parameters must still be met. The two important slider cutting process parameters are chip size and roughness of the cut.

Design of Experiment (DOE) was used to record the effects of the two variables. The results of the DOEs were used to construct a relationship of the two variables on the wear rate, chip size and roughness of cutting surface using response surface method (RSM). The appropriate values of the two variables to be used in production were determined using optimization method.

From the optimization analysis, the most appropriate coolant nozzle angle nozzle is 19.7° and the coolant flow rate is 3.2 gallons per minute (GPM). By implementing two above-mentioned settings, it is possible to extend the life of diamond blade to 25%.

Keywords: dicing with diamond wheel, precision grinding, hard disk drive, slider bar

ACKNOWLEDGEMENT

First, I would like to thank Asst. Prof. Dr. Monsak Pimsarn, my advisor and Mr. Sarapong Choumwong who always provide a lot of sustained guidance, many indispensable advices and reviews. They spend a lot of their time for teaching and discussion. Completion of my thesis may not be achieved without their supports and advices.

Second, I would like to thank my company, Mr. Pricha Leelanukrom who give company scholarship to me and also Mrs. Panita Ngamprasert who supports many things during studying time, I got a lot of good experience and excellent knowledge from data storage technology.

Third, I would like to thank to all DSTAR professors who give me many skills and knowledge. They always welcome for advice and teaching in over time.

Finally, I would like to thank to my family are Mr. Udom, Mrs. Nattaya, Mr. Supasit Manokruang, and Miss Ramon Hirunyalawan that everyone gives unfailing encouragement; especially, my parents. I would like to dedicate this thesis to them and say thank to everyone again for encouraging me to pursue higher education.

Katchamart Manokruang

CONTENTS

CONTENTS (CONT.)

CONTENTS (CONT.)

CONTENTS (CONT.)

LIST OF FIGURES

LIST OF FIGURES (CONT.)

LIST OF TABLES

ABBREVIATIONS

HDD	Hard Disk Drive
SF	Slider Fabrication
HSA	Head Stack Assembly
GPM	Gallon per Minute
DAF	Die Attach Film
AlTic	Alumina Titanium Carbide
DOE	Design of Experiment
ABS	Air Baring Surface
GPa	Gigapascals
CBN	Cubic Boron Nitride
HIP	Hot Isostatically Pressed
DI	Deionized water
P-Value	P-Value probability
RSM	Respond Surface Methodology
SEM	Scanning Electron Microscope
AFM	Atomic Force Microscope
SQP	Sequential Quadratic Programming

NOMENCLATURE

°	Degree
N	Newton
σ	Residual stress
V	Velocity (m/s)
v_c	Cutting speed
F	Force (N)
Δr_s	Radial wheel wear
x	Linear part of the design matrix
$\vec{\beta}$	The vector of linear coefficient
ε	A random experimental error assumed to have a zero mean
θ	Theta
$\vec{c}$	A vector of nonlinear inequality constraints
$\vec{c}_{eq}$	A vector of nonlinear equality constraints
$\underline{A}$	A coefficient matrix of nonlinear constrained equations
$\underline{A}_{eq}$	A coefficient matrix of nonlinear constrained equations
$l\vec{b}$	A vector of lower bound values
$u\vec{b}$	A vector of upper bound values
D_B	Diamond wheel diameter before
D_A	Diamond wheel diameter after
C	Largest edge chip of each SEM image
$\overline{X_1}$	Normalized nozzle angle
$\overline{X_2}$	Normalized coolant flow rate
$\overline{F}_{wear}$	Normalized wear rate function
$\overline{F}_{chip}$	Normalized chip size function
$\overline{F}_{roughness}$	Normalized roughness function
$\overline{F}_{obj}$	Normalized objective function

CHAPTER 1

INTRODUCTION

1.1 Background and motivation

Slider is one of the many components in the hard disk drive assembly. It is basically a head or device to read and write data from and onto the disk. The slider fabrication and dicing are significant processes for slider producing. Abrasive material, known as diamond wheel is required for cutting slider from wafer in head part cut off process as shown in Figure 1.1. Due to being the essential tool and its expensive cost, diamond wheel is major cost of the dicing process.

In order to maintain the industrial competitiveness, cost reduction and/or cost saving is one of the most important factors. Extending the life-time of diamond wheel by reducing the wear rate is one of the effective efforts to pursue cost reduction in dicing process.

Delivering a coolant in a correct direction and area onto the interact part of diamond wheel and slider part (cutting area or heat affected zone) which is functioned as coolant and lubricant, prevents heat transfer resulting in reduction of wheel wear rate. On the other hand, incorrect direction of coolant will increase the heat transfer from cutting area and eventually increase the wear rate of diamond wheel.

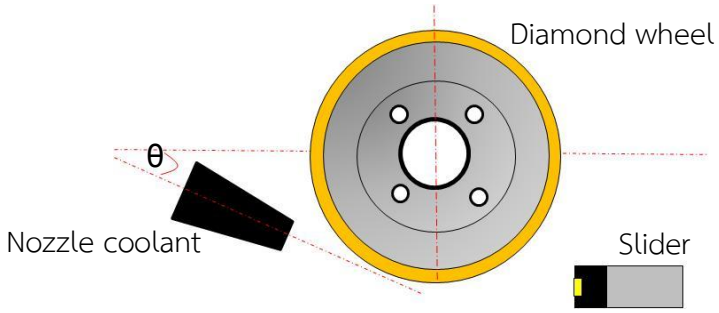

Figure1.1 Schematic of head part process

1.2 Statement of problem

Based on historical data of diamond wheel cost and usage that concerned with diamond wheel wear rate and its biggest cost of indirect material in slider fabrication process, graph of the wear rate tracking was side way trend as shown in Figure 1.2. The graph of diamond wheel life time average was maintaining trend as shown in Figure 1.3 contrarily. In accordance with mentioned data, this study focuses on manufacturing cost improvement for industrial competitiveness.

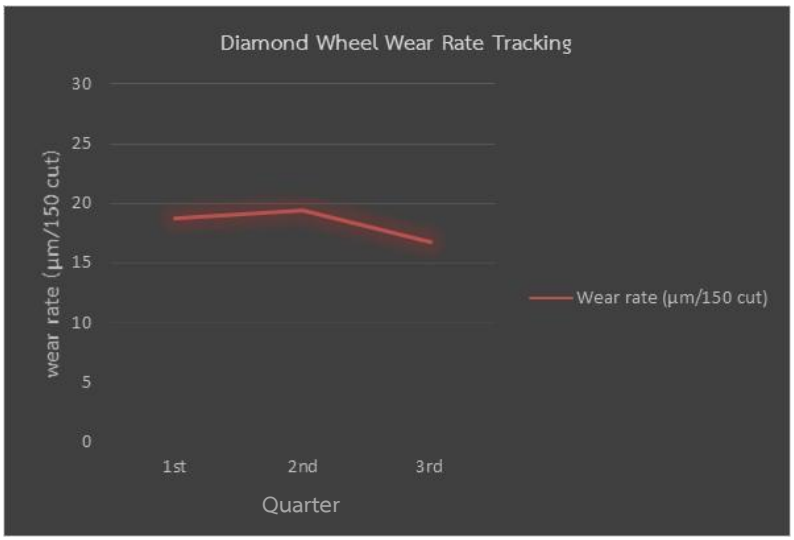

Figure 1.2 Diamond wheel wear rate tracking

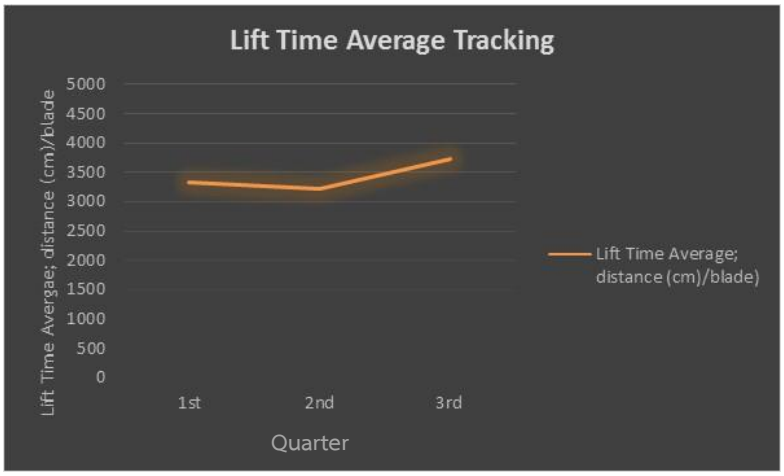

Figure 1.3 Diamond wheel lift time tracking

1.3 Objectives

The objective of this thesis is to study the head part fluid delivery and nozzle angle as the parameters affected significantly to wear rate of diamond wheel and outcome of cutting surface quality. The result of the study allows productive improvement in term of cheaper cost and better quality. The study is divided as three points as follows.

- To study the effect of nozzle angle, coolant flow rate on wear rate, chip size and roughness.
- To find the optimum setting of nozzle angle, coolant flow rate for minimize wear rate, chip size and roughness of cutting surface.
- Validation optimum set points effect to wear rate, chip size roughness and cost saving.

1.4 Assumptions

The thesis focuses on two parameters; coolant nozzle angles and coolant flow rate supply on cutting contacts. Both parameters are used to proceed coolant supply operation with three kinds of indicators; wear rate of diamond wheel, slider edge chip and side wall roughness. Cost and cutting surface quality are improved as well as follows.

- Nozzle angle is operated with coolant supply to cutting zone.
- Coolant flow rate is supplied sufficiently.
- Both factors are affected to wear rate, chip size and roughness.
- Cost saving and cutting surface quality are improved.

1.5 Scope or limitation of study

The study only focuses on head part cut off machine with various types of nozzle angle and coolant flow rates. Other factors including diamond wheel and work piece are controlled variable. AlTiC consisting of a ceramic matrix composited and AlTiC are selected as material of workpiece. The diamond wheel used is SD#2000 (diamond size 10-6 μm). Processing parameter is performed at normal of head part cutting condition.

There are some limitations on this study. First, the types of coolant can be supplied at 3.5 GPM maximum. Second, nozzle is only one shape. Third, space between nozzle and diamond wheel is very close that restricted as a little angle adjustment.

CHAPTER 2

LITERATURE REVIEWS

This chapter focuses on collecting data or information for any machining parameters effecting to wear rate and workpiece surface.

In 1999, S. Ebbrell, et al. [1] studied the effect of nozzle position of supplying grinding fluid effect to workpiece surface qualities by three different nozzle positions experiment; angular, intermediate and tangential position as shown Figure 2.1. They were measured in power of grinding with workpiece surface quality by arithmetic mean surface roughness (Ra) and size scatter by light scattering by particle that is defined by size parameter which is the ratio of its characteristic dimension. According to experiment, the angular position was better on Ra (0.5 μm) as shown in Figure 2.2 and size scatter met target (5 μm) as shown in Figure 2.3 which could be concluded that the nozzle position affected to workpiece surface qualities in term of Ra and scatter for the target size.

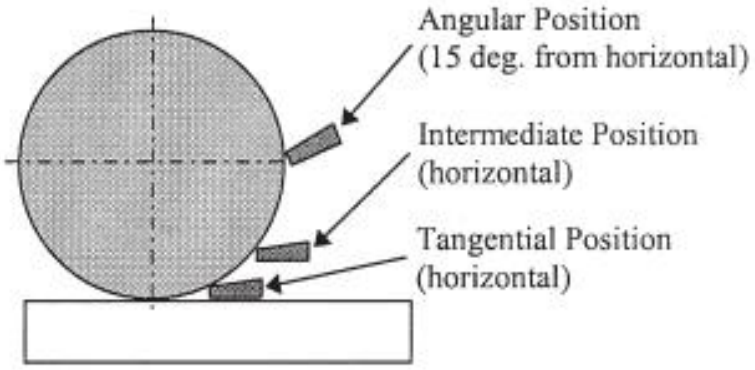

Figure 2.1 Nozzle positions [1]

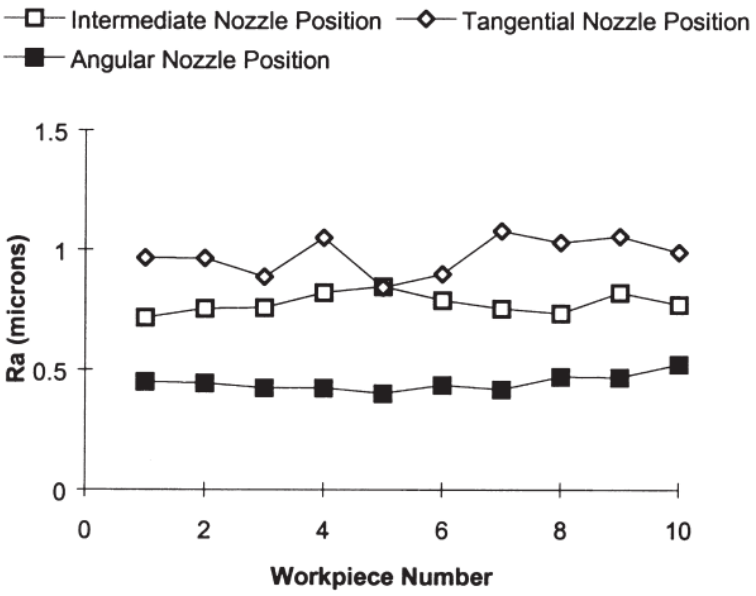

Figure 2.2 Workpiece Ra [1]

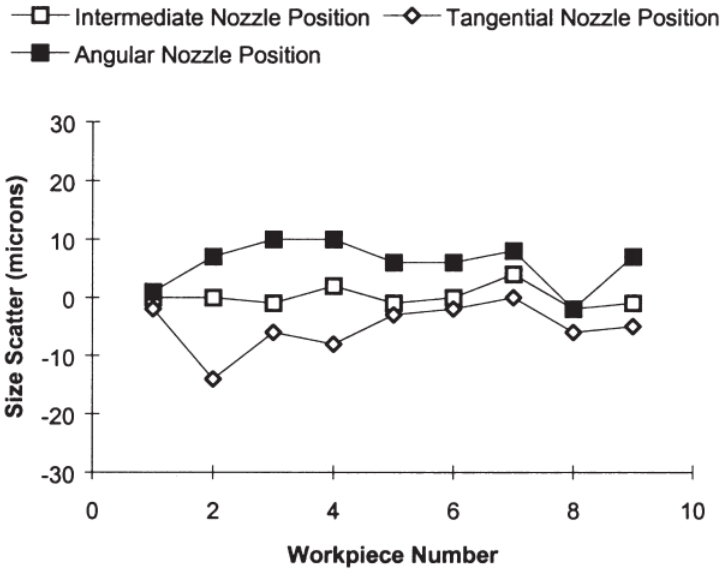

Figure 2.3 Workpiece scatter [1]

Hans H. Gatzen and Jeihad Zeadan [2] studied the investigation on coolant supply in precision dicing and suggestion as new technique to investigate ability of coolant achieved passing through cutting zone as shown in Figure 2.4 (the conventional

approach to determine the volume flow using a guide blade behind the wheel to collect the coolant) showing the schematic of approach taken, a workpiece holder was equipped with groove with a progressive depth. A bore in the groove serving as an exit orifice was connected to external duct (tube). The duct observed percentage of air bubbles. A groove was ground into the workpiece and then it was glued to the workpiece holder with both channels formed by the respective grooves line up. During a test cut, the groove was cut open which then allowed collecting the coolant flowing through the cutting zone. Then investigate coolant flow rate are affect to cutting forces that found increasing the flow rate obtain the cutting force to decrease as shown in Figure 2.5. That would be assisting to improve cutting load, heat transfer and cleaning the swarf.

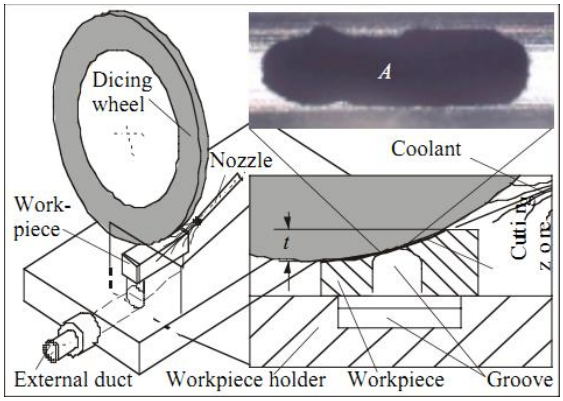

Figure 2.4 Schematic of measure coolant flow in cutting zone [2]

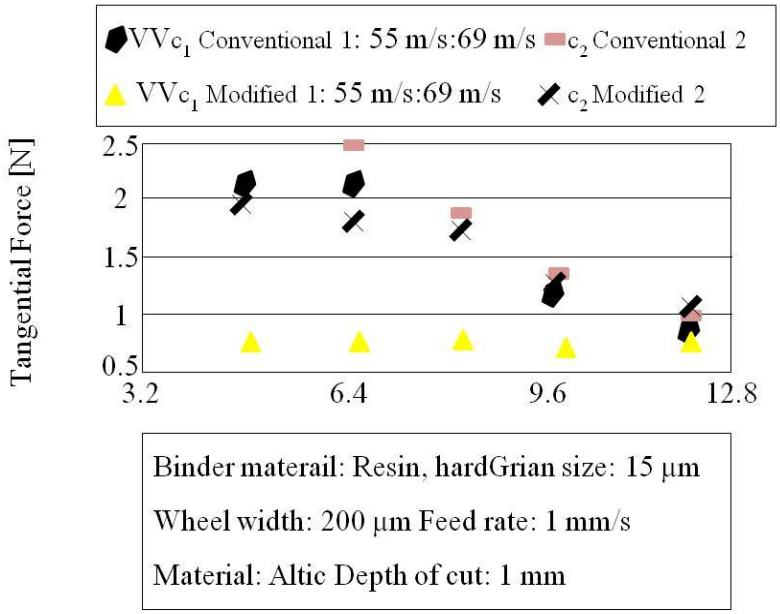

Figure 2.5 Cutting force (y-Axis) as nozzle jet velocity (x-axis) [2]

In 2006, Hoh Huey Jiun, et al. [3] studied Die Attach Film (DAF) wafer dicing process as shown in Figure 2.6 effecting to character of chip/crack and roughness of workpiece. The experiment was performed by changing three types of die consist of bare silicon die no-laminate, nonconductive DAF-laminated die and conductive DAF-laminate die effecting to chip and roughness which were characterize by hi power scope and Atomic Force Microscopy (AFM) accordingly. The results were shown that die film effected to size chip/crack and roughness by bare silicon die no-laminate given minimize of chip/crack and roughness as shown in Figure 2.7 and 2.8.

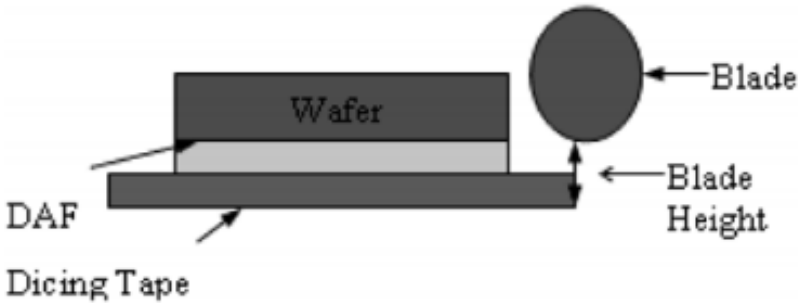

Figure 2.6 Dicing illustrate [3]

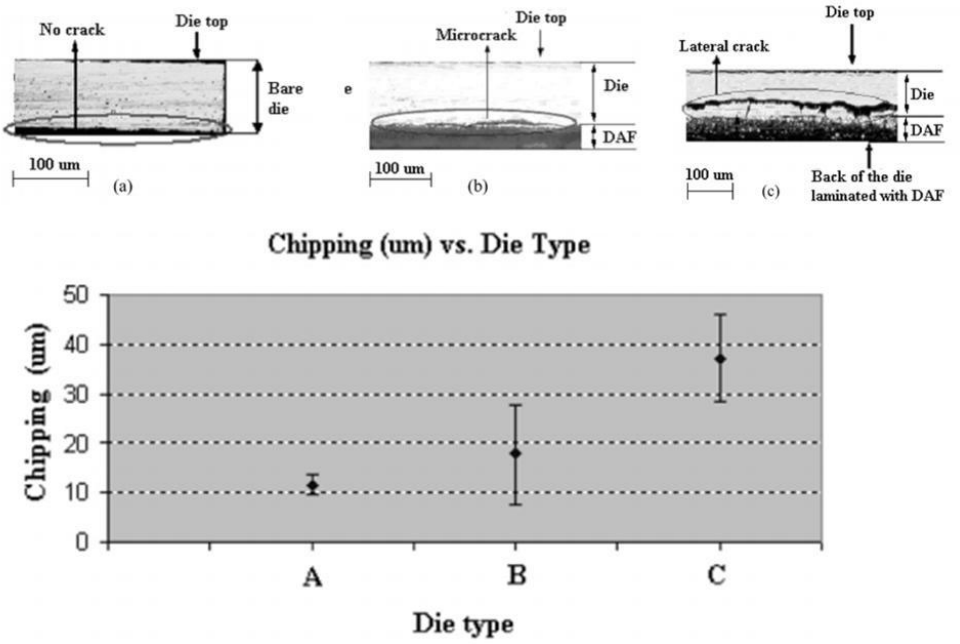

Figure 2.7 Comparison of chip/crack condition [3]

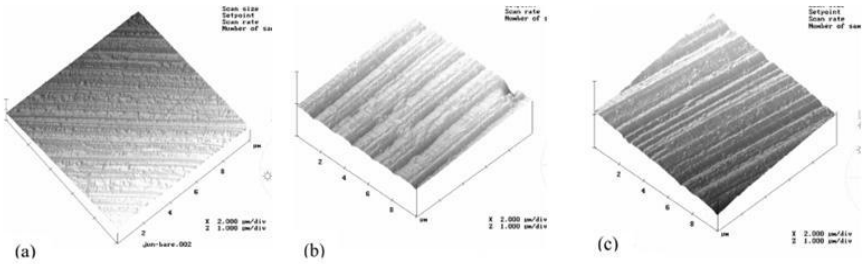

Sample Diced Surface	Ra (nm)
Bare silicon - Non-laminated (A)	10.901
Non-conductive (B)	13.775
Conductive laminated (C)	17.404

Figure 2.8 Comparison of Ra condition [3]

In 2006, W.Li, et al. [4] studied the influence depth of cut of diamond wheel each diamond grit size number are 80 (45 μm), 180 (30 μm) and 400 (8 μm) on wear of diamond abrasive and material removal rate. The results were shown that there was an optimum depth of cut ($4x10^{-4}$ m), which was greatest material removal rate. If the depth of cut was less than the optimum depth of cut the grinding to low affective as shown in Figure 2.9. If the grinding depth was larger than the optimum, the diamond wheel lift would be early as shown in Figure 2.10.

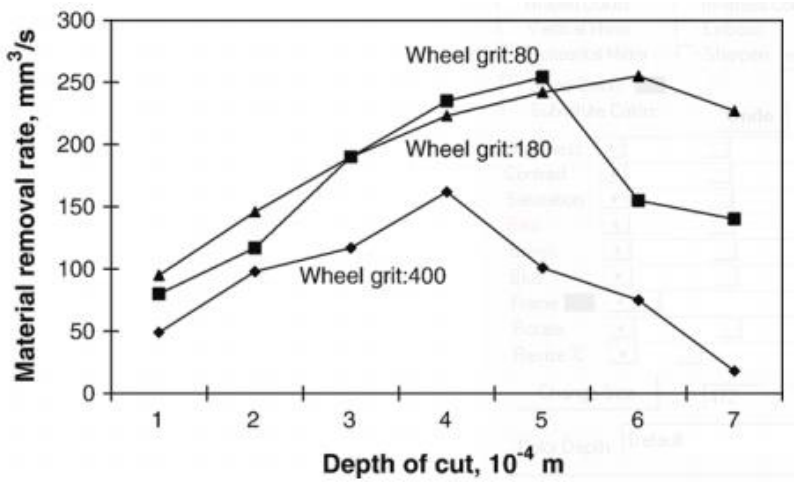

Figure 2.9 Comparison depth of cut vs. material removal [4]

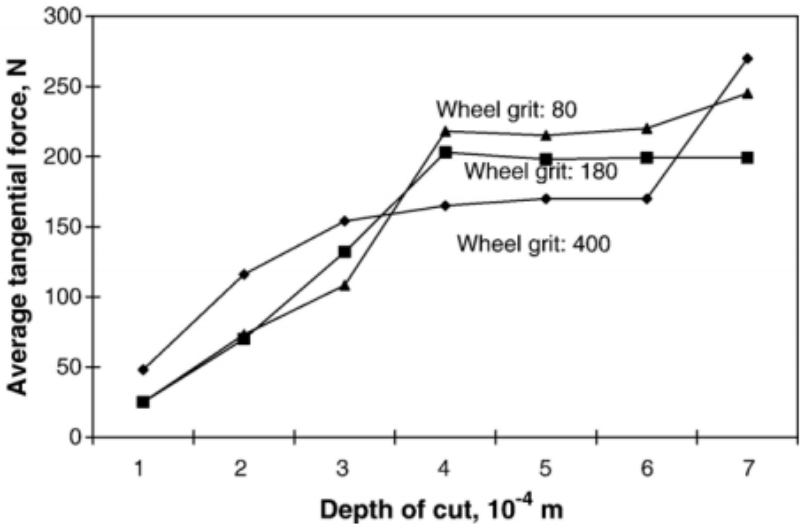

Figure 2.10 Comparison depth of cut vs. avg. tangential force [4]

In supplied lubrication to workpiece. Nozzles were designed to main factor effect to thermal and lubricant at cutting area. Besides flow coolant are also affected. Efficiency of thermal and lubricant can be indicator by residual stresses. Czenkusch, et al. [5] found that effect of coolant flow rate increased, varying form 0 – 7 l/(min mm) and diameter of nozzle outlet as shown in Figure 2.11. There are 7.5 mm^2 (white triangle), 15 mm^2 (black circular), 30 mm^2 (black triangle), 45 mm^2 (black square) and 60 mm^2 (back diamond) to residual stress at the workpiece. Their results shown, increasing coolant flow rate of each outlet cross section obtained different residual stresses. The nozzle 7.5 mm^2 has provided the less of residual stresses. Other nozzle, residual stresses were reduced when coolant flow rate were increased.

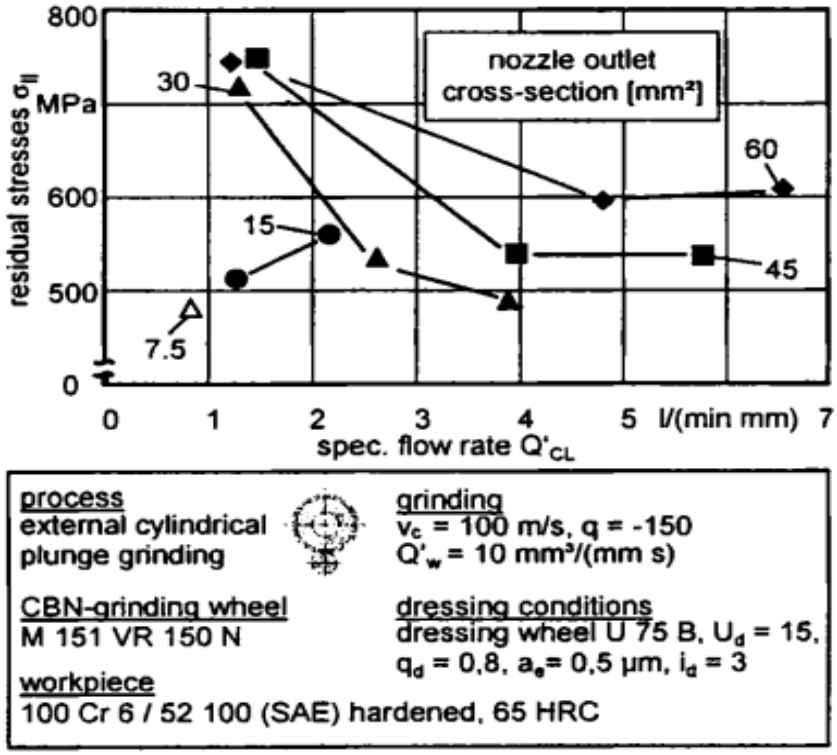

Figure 2.11 Effect of flow rate and nozzle cross section on residual stress [5]

Another one factor have effected to efficiency of workpiece surface quality. That is coolant properties. In 1998, Weinert, et al. [6] had done the experiment to study the

effect of emulsion, graphite used in lubrication and dry supplied in grinding process and varying spec of removal rate. Observation on arithmetic mean surface roughness (Ra) of workpiece and radial wheel wear (Δr_s). Their results shown relationship of spec of removal rate and mixer affected to surface roughness and radial wheel wear. By graphite mixed was obtained better Ra and radial wheel wear but varied as spec of removal rate also as shown in Figure 2.12.

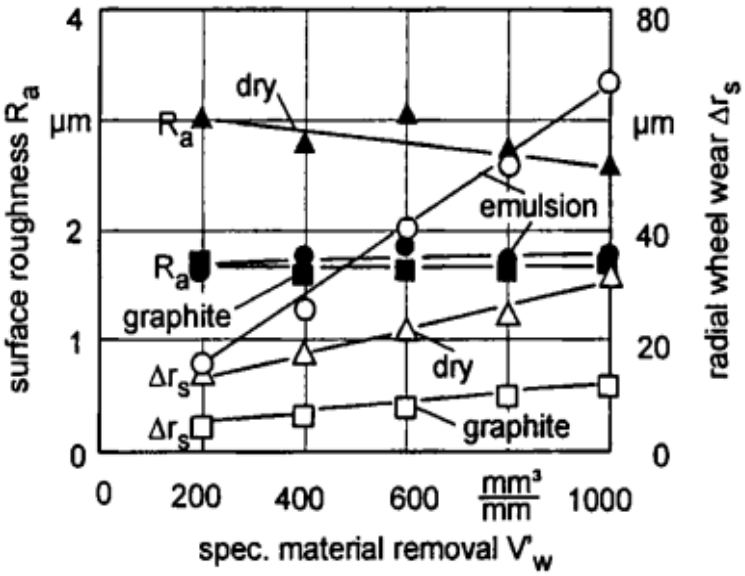

coolants: ● ○ emulsion 4%; ▲ △ dry; ■ □ graphite	
grinding wheel:	38A46 I 8 VS
cutting speed:	v_c = 25 m/s
depth of cut per pass:	a_e = 15 μm
table speed:	v_{ft} = 21 m/min
spec. mat. rem. rate:	Q'_w = 5.25 mm³/(mm s)
workpiece material:	100 Cr 6 / 52 100 (SAE) (750 HV 10)

Figure 2.12 Influence of coolant types [6]

As in literature review, it can be concluded that shown coolant position, coolant flow rate, dept of cut, nozzle type and coolant type effecting to cutting force which is the root cause of wear rate and workpiece surface qualities.

CHAPTER 3

RELATED THEORIES

This chapter concerns the theories as follows.

- Head Part off Process
- Abrasive Process
- Basic of Grinding Process
- AlTiC Material Properties
- Fluid Process
- Statistic
- Respond Surface Methodology (RSM)
- Multi variable optimization with inequality constraints

3.1 Head part process

In Hard Disk Drive (HDD) manufacturing, there are three main operations with Slider Fabrication (SF), Head Stack Assembly (HSA) and HDD assembly as shown in Figure 3.1 and 3.2. The slider fabrication is operation to make read/write head (slider) of HDD. Head part process is a part of slider fabrication as shown in Figure 3.3 which cut the row bar into slider form.

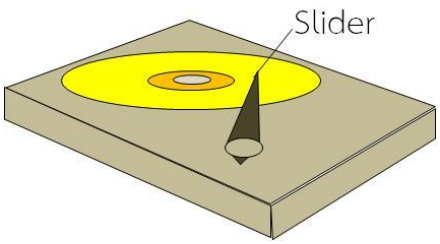

Figure 3.1 Slider in HDD

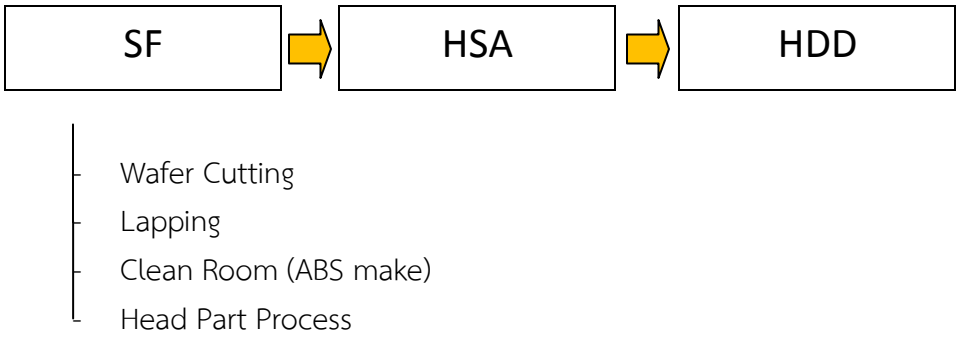

Figure 3.2 Three main operations in HDD manufacturing flow

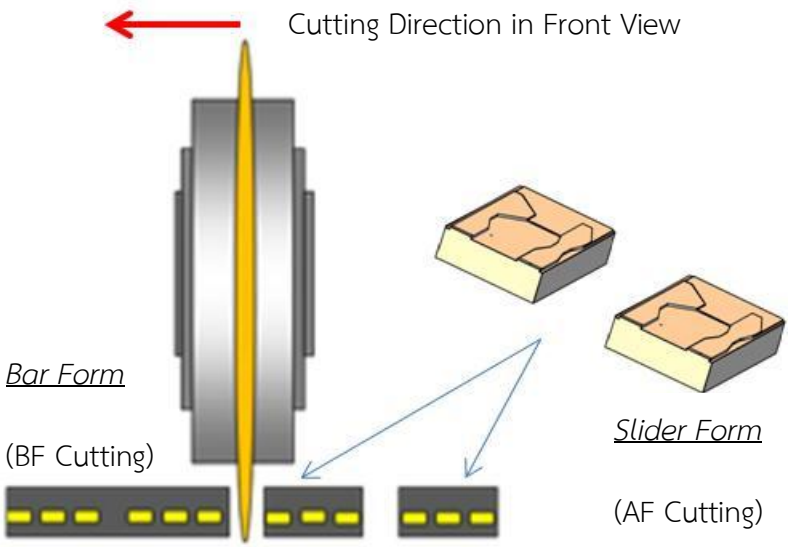

Figure 3.3 Head Part Process

3.2 Abrasive process

Abrasive machining processes are manufacturing techniques working on hard material to modify the shape and surface texture of manufactured parts. Abrasive process is used for produce high quality, high accuracy and surface texture of parts [7].

Most of abrasive process can be separated into four groups as shown in Figure 3.4:

1) Grinding; Abrasive tool is a grinding wheel which moves at a high surface speed comparing to other machining processes. The speed of grinding wheel moves up to 140 m/s on high speed grinding.
2) Honing; Abrasive particles or abrasive grains are fixed in bonded tools. This process is mainly used to finish surface in bore of cylinder.
3) Lapping; Free abrasive particles are between lap plate and workpiece surface. The abrasive is usually suspended in liquid.
4) Polishing; Although it is mostly similar to lapping process, the difference is forming hard plate into soft cloth pad.

Main purpose of grinding is modifying shape of workpiece, however polishing is modifying surface texture of workpiece.

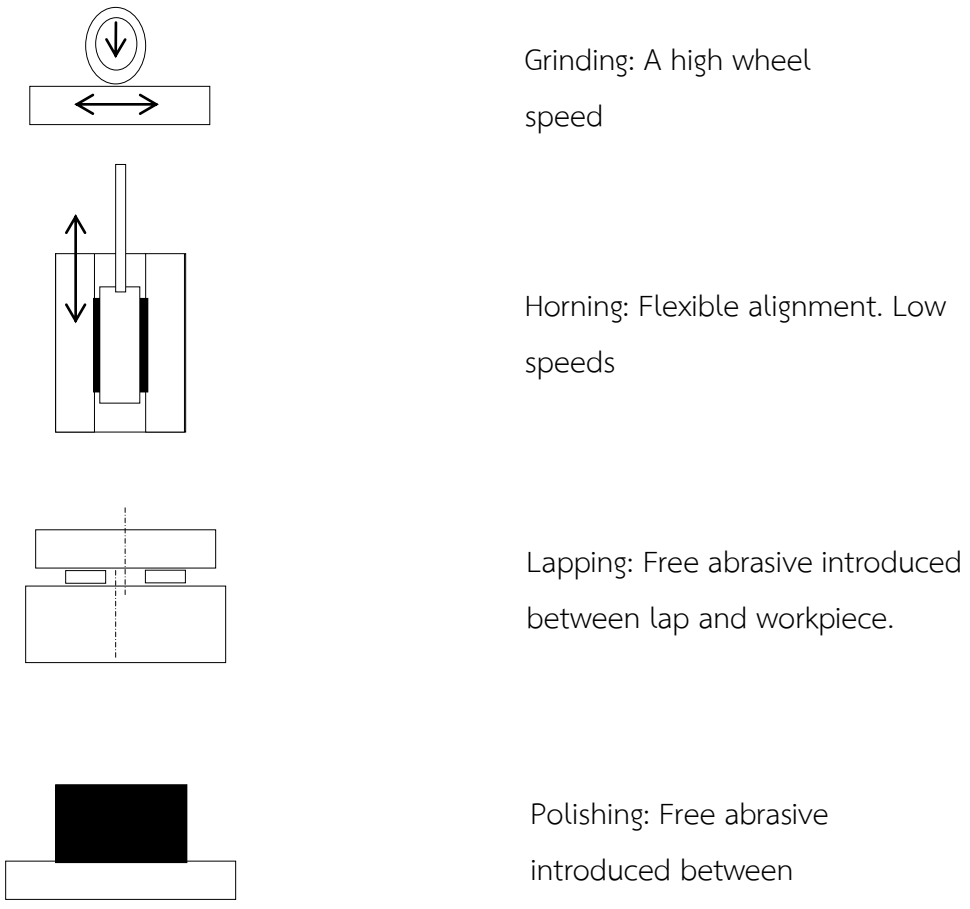

Figure 3.4 Basic principles of grinding, honing, lapping, and polishing [7]

3.3 Basic of grinding process

Grinding process consists of six basic elements combining in system as shown in Figure 3.5 shown.

1) Grinding machine
2) Grinding wheel
3) Work piece
4) Grinding fluid
5) Atmosphere
6) Grinding swarf

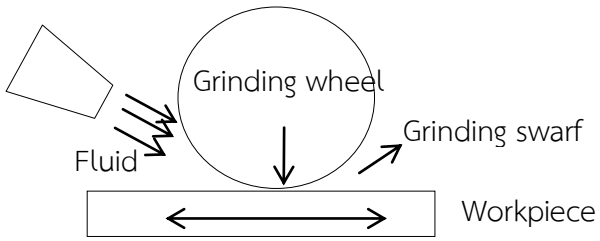

Figure 3.5 Six basic elements involved in surface grinding [7]

3.3.1 Type of grinding operation

Grinding can be separated into 4 basic operations using straight wheel as shown in Figure 3.6.

1) Peripheral surface grinding
2) Peripheral cylindrical grinding
3) Face surface grinding
4) Face cylindrical grinding

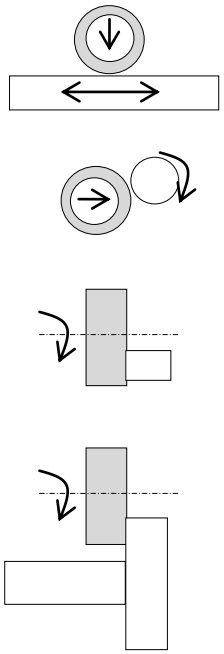

(a) Peripheral surface grinding

(b) Peripheral cylindrical grinding

(c) Face surface

(d) Face surface grinding

Figure 3.6 Four basics grinding operations using straight wheels [7]

3.3.2 Type of abrasive

In abrasive machining process, grain of abrasive must be harder than workpiece. It must be under high temperature condition abrasive grain to maintain harder character than work piece also. De Beers, showed hardness value of abrasive grain in Table 3.1.

Table 3.1 Typical hardness values of abrasive grain material

Units	Vickers hardness (GPa)
Diamond	56-102
Cubic boron nitride (CBN)	42-46
Silicon carbide	~ 24
Aluminium oxide	~ 21
M2 tool steel (double tempered)	~ 0.81

3.3.3 Diamond wheel

It is an abrasive tool which abrasive layer is the main component with a composite structure including grit. The abrasive layer made up from hard abrasive grit and bond material to retain the grit within tridimensional structure, and held or attached

in a tool holder. The main contact was between tool surface and workpiece taking place on the hard and sharp edge of the grit. The hardness of grit is sufficient to plastically deform the workpiece material. [8]

Diamond grit can be explained and converted into standard definition to diamond grain size as in Table 3.2.

Table 3.2 Diamond grit size convert table

Regular Micro Mesh	MicroMesh MX	Micro-Mesh AL	Grit (US)	Microns	Inches
		300	180	80	0.0030
	60		230	60	0.0024
	80		280	45	0.0018
	100	600	320	40	0.0016
	150	800	360	35	0.0014
1500	180	1500	400	30	0.0012
1800	240	1800	600	15	0.0006
2400	320	2400	900	12	0.0005
3200	360	3200	1200	9	0.0004
3600	400	3600	1350	8	0.0003
4000	600	4000	1500	5	0.0002
6000	800	60010		4	0.0002
8000	1200	8000		3	0.0001
12000		12000		2	0.0001

3.3.4 Tribological system

The system investigation of a tribological system requires inputs and outputs consideration. Figure 3.7 shows the nature of the inputs being considered.

The inputs and outputs can be broken down into motion, material, energy and information. In a detailed analysis, each of these categories is examined to determine its influences on the process. In addition, there are disturbances to the process such as vibrations which may, in a few cases, be controllable, but not always avoidable.

There are also outputs from the process which may be considered as losses. These include frictional losses and wear products. Some of the factors to be considered in an abrasive machining process are illustrated as shown in Figure 3.8.

In the following chapters, the important elements of the abrasive machining system and tribological factors that control the efficiency and quality of the process are considered. Since grinding is by far the most commonly employed abrasive machining process, it is described in detail.

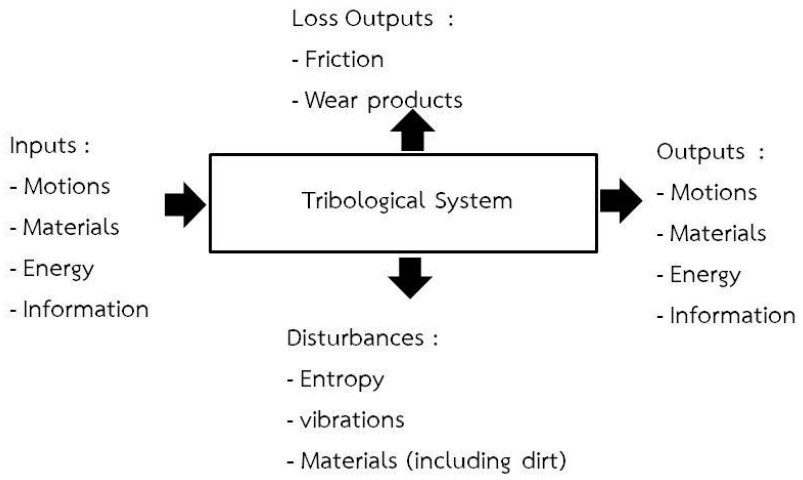

Figure 3.7 Inputs and outputs of Tribological system [7]

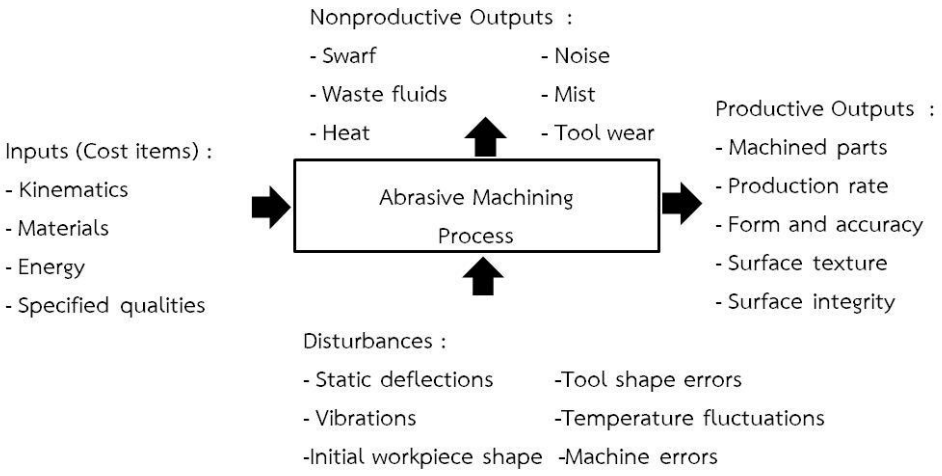

Figure 3.8 Inputs and outputs of abrasive machining processes [7]

Summaries of the tribology system as shown in Figure 3.9 was on the effects of coolant lubrication and cooling respectively that shown influence to tool wear, force and power demand.

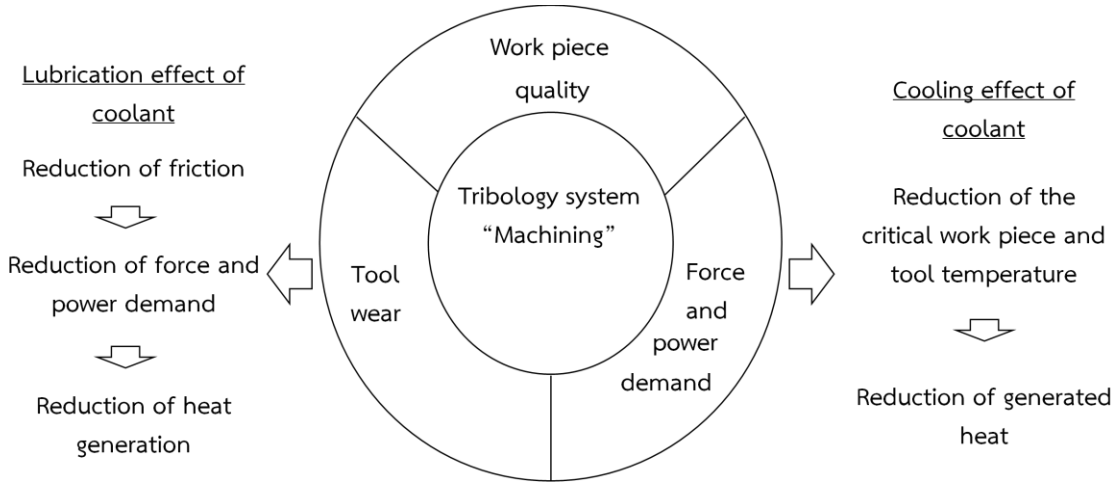

Figure 3.9 Tribology system effects by lubrication and cooling [9]

3.4 AlTiC material properties

The main material of slider head is AlTiC material. AlTiC is stand for Alumina-Titanium Carbide produced by hot isostatically pressed (HIP). AlTiC is high density ceramic materials with a porosity.

3.5 Grinding fluid

The main purpose of a grinding fluid is to minimize mechanical, thermal, and chemical impact between the active partners of the abrasive process. Grinding fluid used for cooling and lubricating in grinding process.

Basic requirements of a grinding fluid are good lubrication, good cooling and flushing performance and high corrosion protection. Secondary requirements of grinding fluid are economic and efficient operation, operational stability (long life) and environmental protection.

3.5.1 Types of grinding fluid

- Water-immiscible cooling lubricants; are not generally mixed with water for any application.
- Water-miscible cooling lubricants; are emulsification or water-soluble concentrates, to which water is added before use.
- Water-composite cooling lubricants; are ready-for-use composites of water-miscible cooling lubricants with water, within the group of water-miscible cooling lubricants.

3.5.2 Head part coolant

Head Part coolant is synthetic metal mixed with DI water and working fluid specifically for diamond wheel grinding. It provides outstanding cooling, rapid fine setting and exceptional wetting with dry film corrosion protection for workpieces and machine and its transparent fluid.

3.6 Tool wear

Wear is generally defined as a mechanical damage to a solid surface, generally involved progressive loss of material, due to relative motion between the contacting surfaces. The wear can be divided into mechanism type as follows.

1. Abrasive wear
2. Friction
3. Fatigue
4. Erosion

3.7 Chip on material

Heating of the surface is accompanied by thermal expansion and contraction. The wheel passes a point on the work piece. The surface expands due to heating. After the wheel has passed, the surface rapidly cools and is quenched by the mass cooling from the subsurface. At this stage the material contracts as shown in Figure 3.10.

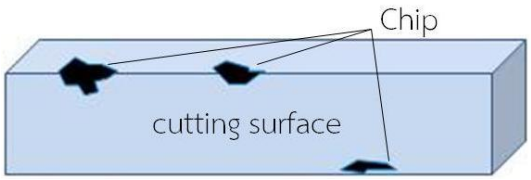

Figure 3.10 Sample of Chip

3.8 Roughness

Surface topography is great importance in specifying the function of a surface finish after grinding surface. In the manufacturing industry, basic requirement of process is good surface finish and surface must be within certain limits of roughness requirement of process. Ra and Rz is the most useful parameter to identify the surface roughness after machining process

Ra (Arithmetic mean surface roughness): A section of standard length is sampled from the mean line on the roughness chart as shown in Figure 3.11.

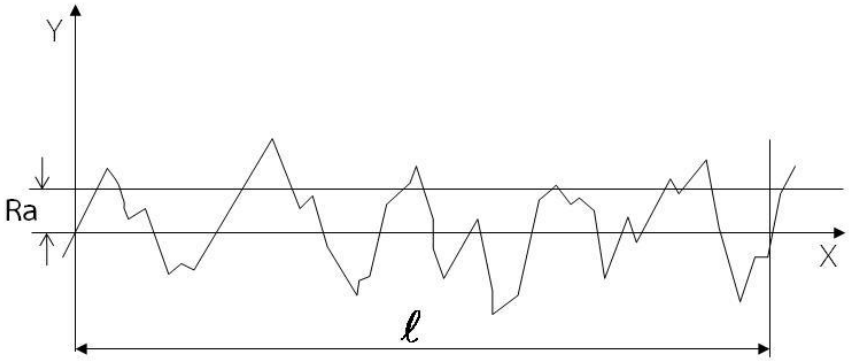

Figure 3.11 Arithmetic mean surface roughnesses (Ra)

$$Ra = \frac{1}{\ell}\int_{0}^{\ell} |f(x)|dx \qquad (3.1)$$

3.9 Design of Experiment (DOE)

In 1920, Ronald Fisher was developer on Design of Experiment method (DOE) and applied in agriculture. A method of DOE was used to indentify significant factors, correct and possibility estimated interaction in process [10].

Design of a series structure test to forecast the changes of input variables is the process which effects of whole changes on a defined output after assesses. Using the tool starts for order tasks by identifying the input variables and output which can be measured. A number of levels are defined each input variables which presents the range for that effect to desired variables. The produced experiment plan and setup parameter are preceded on the best.

3.9.1 Factorial designs

Factorial design is the study of several factors that have an effect to a process at the same time when performing an experiment. Factor levels are varied simultaneously rather than one at a time that is efficient in term of time and cost allowing the study of interactions between the factors also. Interactions are the driving force without factorial experiments in many processes while important interactions may remain undetected.

All combination of experimental factor levels is measuring in responses of a full factorial representing the conditions that were measured. According to the experiment, experiment of each condition is called as “run” with the response measurement observation. Whole set of runs is called as “design”. The following diagrams show two and three factors design. Each point are represented a unique combination of factor levels. As in two-factor design, the point on the lower left corner represents the experimental run when Factor A is set at its low level and Factor B is also set at its low level (as shown in Figure 3.12-3.13).

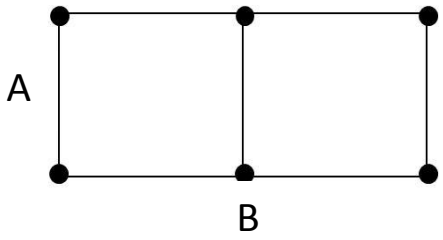

Figure 3.12 Two levels of factor A and three levels of factor B

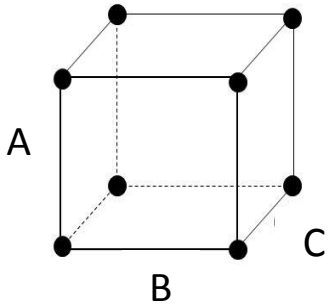

Figure 3.13 Two levels of three factors

3.9.2 Factorial plots (General full factorial)

General and full are two types of factorial plots design those help to visualize the main effects and interactions. Both plots can be used to show how the variables response to one or more factors.

3.9.3 Main effects plot

Main effects plot is generally a plot each factor level mean. When the factor level alters, it causes altering of output variable and occurring of main effects. The following main effect plots are applied to compare the relative strength of effects with factors. Graph plotting of main effect is demonstrating in line. A horizontal line shows that each factor level existing doesn't affect the response correspondingly. The response mean is same across whole factors levels when the line is not in horizontal position. Moreover, different levels of the factor affect the response differently. The less horizontal line showing greater likelihood as main effect is statistically significant as shown in Figure 3.14.

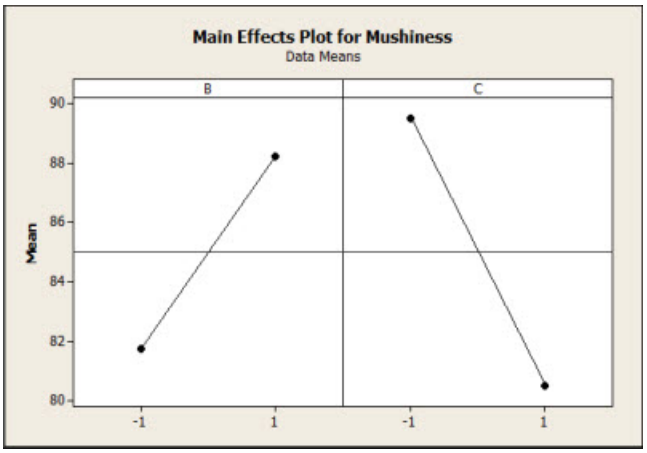

Figure 3.14 Graph window output of main effects plot

3.9.4 R-square

Based on comparing the variability of estimation errors with the variability of the original values

$$R^2 = 1 - \frac{SS_{res}}{SS_{tot}} \tag{3.2}$$

Where SS_{res} is sum of squares of residue and SS_{tot} is total sum of square.

- Percentage of response variation is explained with one or more possible relations.
- In general, higher the R-square improves the better results of data model.
- R^2 always increases as number of predictors increase and reaches to maximum when p=k
- As R^2 is maximum at p=k, it is not a proper indicator for model improvement.

3.9.5 P-Value probability (P-Value)

P-Value is taken to determine whether a factor is significant; typically comparing with an alpha value of 0.05. If the p-value is lower than 0.05, the factor will be significant. The sample of probability model is as shown Figure 3.15.

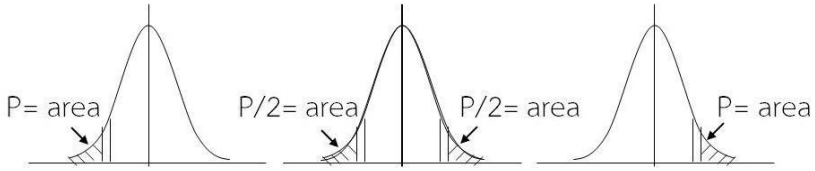

Figure 3.15 Probability model

3.10 Response Surface Methodology (RSM)

In 1951, Box and Wilson introduced Response Surface Methodology (RSM) on a series of experiment, analysis and optimization techniques. [11] That idea was optimization an unknown and noisy function by means of simpler approximating functions that were valid over a small region using designed experiments.

They suggested using a first degree polynomial model to approximate the output variables (response). Anyway the model was only an approximation which was not accurate but easy to estimate and apply when few was known on process. The second order models were many subject occur, engineers and scientists had working knowledge of the central composite design (CCDs) and Box and Behnken design three level in 1960.

The RSM consists of a group of mathematical and statistical techniques using in the development of an adequate functional relationship between response y and a number of input variables which denoted by $x_1, x_2, ..., x_k$. An unknown relationship can be approximated by a low degree polynomial model below.

$$y = f(x_1, x_2) + e \tag{3.3}$$

The variables x_1 and x_2 are independent variables when the response y is upon them. The independent variable y is a function of x_1, x_2 and the experiment error term denoted as e. The error e term is represented to any error measurement on the

response. Other kind of variations in f total is a statistical error being excluded and assumed to distribute with zero mean and variance s^2 normally.

There are two main models commonly using in RSM. They are special model including first order model with 2 independent variables that can be expressed as per below.

$$y = \beta_0 + \beta_1 x_1 + \beta_2 x_2 + \varepsilon \tag{3.4}$$

Where x is linear part of the design matrix, $\vec{\beta}$ is the vector of linear coefficient and ε is a random experimental error assumed to have a zero mean.

The curvature of response surface after a higher polynomial degree can be used for approximate function with two variables called second order model.

$$y = \beta_0 + \beta_1 x_1 + \beta_2 x_2 + \beta_1 x_1^2 + \beta_2 x_2^2 + \beta_{12} x_1 x_2 + \varepsilon \tag{3.5}$$

Basically, all of RSM problems are either one or combined of the both models. The each factor levels were independent from each factor levels in each model. According to the most efficient results in approximate of polynomials, the absolute experimental is designed for data collecting. When the data is collected, the response surface analysis is shown by the fitted curve. The objective of considered model is finished by following factor.

1. Model of relationship between y and $x_1, x_2, ..., x_k$ can be used to predict response values for given setting of the control variables.
2. Hypothesis testing is used in determining the significance of the factors levels represented by $x_1, x_2, ..., x_k$.
3. Optimum setting of $x_1, x_2, ..., x_k$ determining results in the maximum or minimum response over a certain region of interest.

3.11 Sequential Quadratic Programming (SQP)

SQP is an iterative method for nonlinear optimization. SQP method is used on problems for which the objective function and the constraints are twice continuously differentiable.

SQP method solves a sequence of optimization subproblems, each of which optimizes a quadratic model of the objective subject to a linearization of the constraints. If the problem is unconstrained, then the method reduces to Newton's method for finding a point where the gradient of the objective vanishes. If the problem has only equality constraints, then the method is equivalent to applying Newton's method to the first-order optimality conditions, or Karush–Kuhn–Tucker conditions, of the problem. SQP method has been implemented in many packages, including NPSOL, SNOPT, NLPQL, OPSYC, OPTIMA, MATLAB, GNU Octave and SQP.

3.12 Multi variable optimization with inequality constraints

Since Inequality constraint is mostly common in optimization problems. The most common kind of inequality constraints are simple bounds which the variables is satisfied. [12] The constraints optimization problem of many variables subjected to constraints is as following.

$$\text{Minimize} \quad f(x_1, x_2, ..x_n) \tag{3.6}$$

$$\text{Design variables} \quad \vec{x} = [x_1, x_2, ..., x_n]^T \tag{3.7}$$

$$\begin{aligned} &\vec{c}(\vec{x}) \le \vec{0} \\ &\vec{c}_{eq}(\vec{x}) = \vec{0} \\ \text{Subject to} \quad &\underline{A} \bullet \vec{x} \le \vec{b} \\ &\underline{A}_{eq} \bullet \vec{x} = \vec{b}_{eq} \\ &l\vec{b} \le \vec{x} \le u\vec{b} \end{aligned} \tag{3.8}$$

Where

$\vec{c}$ is a vector of nonlinear inequality constraints.

$\vec{c}_{eq}$ is a vector of nonlinear equality constraints.

$\underline{A}$ is a coefficient matrix of nonlinear constrained equations.

$\underline{A}_{eq}$ is a coefficient matrix of nonlinear constrained equations.

$l\vec{b}$ is a vector of lower bound values.

$u\vec{b}$ is a vector of upper bound values.

Graphical optimization

The graphical solution can be used to study in field of minimization problem. Programming techniques are useful in finding from minimum function of several variables under a prescribed set of constraints. Moreover an optimization problem having only two design variables can be solved by observing the way they are graphically represented [13].

CHAPTER 4

EXPERIMENTAL PROCEDURE

This chapter concerns about experimental procedure as follows.

- Material Preparation
- Type of Instrument
- Tooling Fixture
- Bar Bonding Prior Experimental
- Experimental Parameter
- Measurement
- Experimental Analysis
- Optimization Setup

4.1 Materials preparation

The materials were used in the process are as follows.

4.1.1 Row bar

Row bar was cut from AlTiC substrate wafer which was wafer. The wafer was cut in standard row bar.

4.1.2 Diamond wheel

New diamond wheel was prepared by initial dressing prior experiment. It was cut to control kerf and prepared asperity of diamond contact.

4.1.3 Coolant

Coolant was used as lubricant and cooling fluid in cutting process, by mixing with DI water in 1:20 liters ratio with 15°C temperature controlled.

4.1.4 Dressing stone

Dressing stick was prepared before using by soaking in the coolant about 15 min.

4.2 Instruments

Table 4.1 List of experiment instruments

Instruments	Function of Work
Head Part machine	Three axis dicing machine
Atomic Force Microscope (AFM)	Surface roughness measurement
Scanning electron microscope (SEM)	Produce images of a sample by scanning

4.3 Tooling fixture

4.3.1 Head part fixture

Head part fixture was produced from stainless that could contain many row bars/fixture. It was attached to many row bars in a fixture for faster cutting.

4.3.2 Coolant nozzle

Coolant nozzle used is original designed.

4.4 Row bar bonding on head part fixture

All row bars were prepared before cutting experiment by putting on the fixture as following steps.

4.4.1 Applying wax on head part fixture

This step is applying wax before attaching the row bar to the fixture as shown in Figure 4.1.

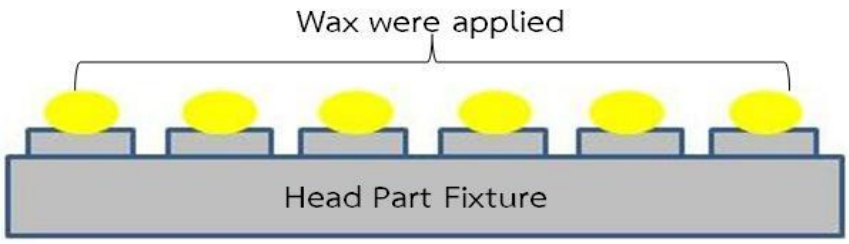

Figure 4.1 Applying wax on head part fixture before row bar bonding

4.4.2 Row bar alignment

All row bars were attached to the fixture and then arranged to strength by marker of each one as shown in Figure 4.2.

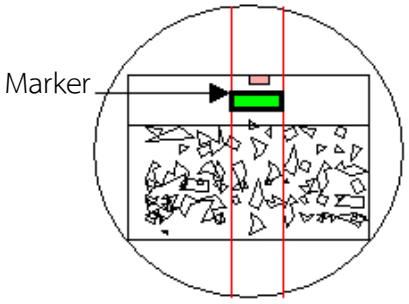

Figure 4.2 Alignment row bar

4.4.3 Cooling down

This step is to leave the attached fixture at room temperature for few minute to allow wax curing holding with row bar on cutting positioning. The overview flow is presented as shown in Figure 4.3.

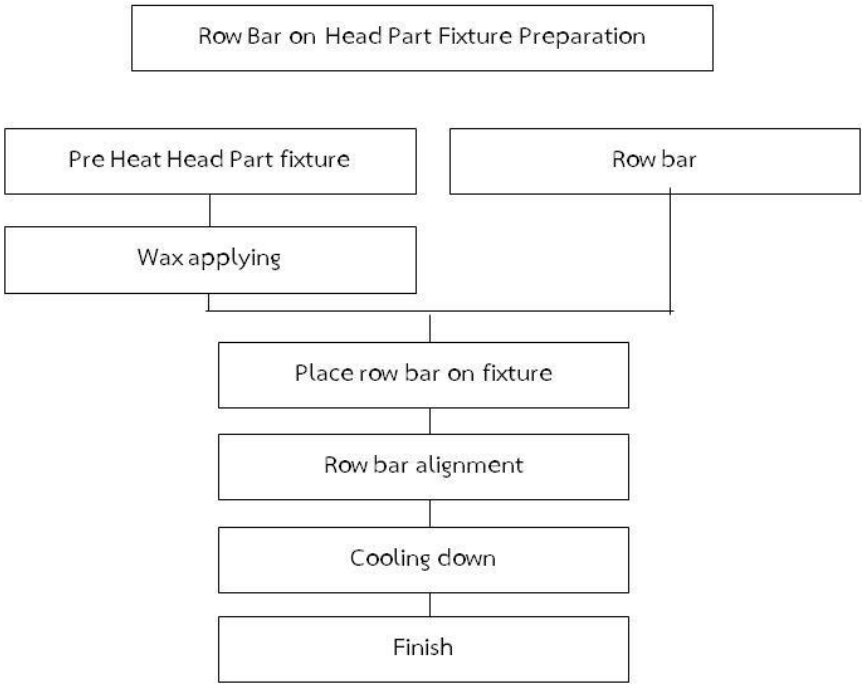

Figure 4.3 Overview flow of row bar on head part fixture preparation

4.5 Head part cutting parameters

Proceeding head part fixture into cutting as condition settled in current condition.

4.6 Experimental parameter

4.6.1 Nozzle angle adjustment

The nozzle was adjusted angle on three angle which this experiment are 18°, 20°

and 22° as shown in Figure 4.4.

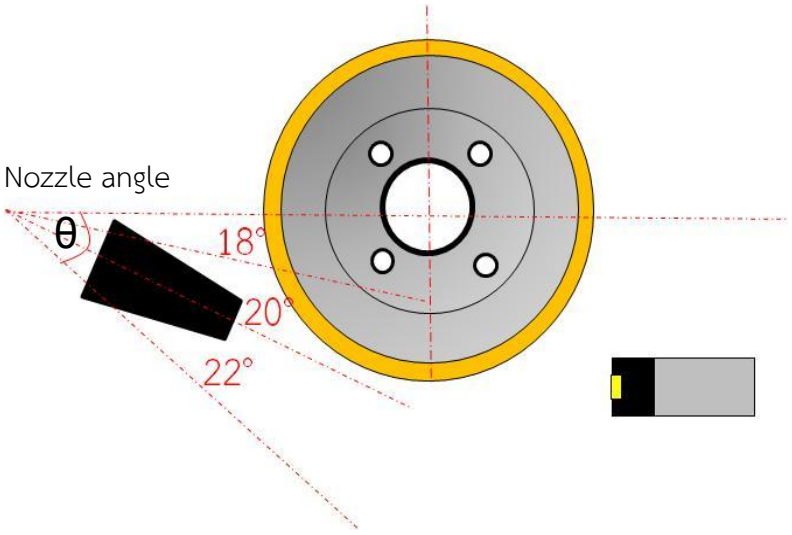

Figure 4.4 Adjusting nozzle angle by various experiments

4.6.2 Coolant flow rate adjustment

Coolant flow rate was adjusted by the coolant valve inlet of the nozzle is 2 GPM, 2.3 GPM and 3 GPM as shown in Figure 4.5. The machine was available coolant flow between 0 to 3 GPM and resolution adjustment 0.5 GPM.

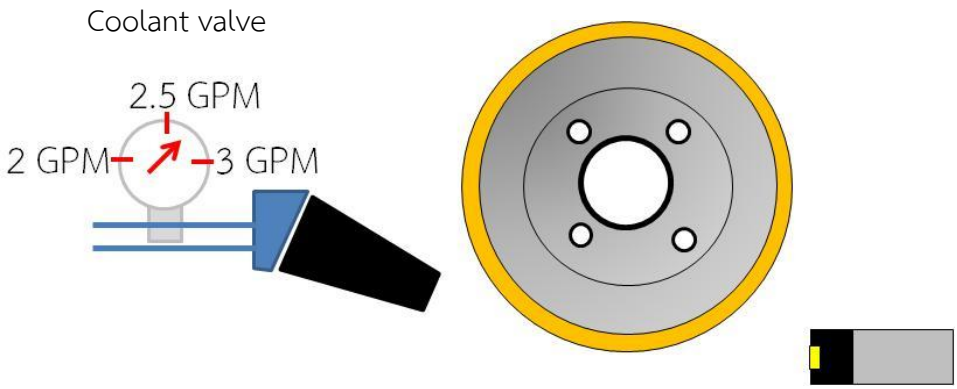

Figure 4.5 Adjustment of coolant flow rate

4.7 Measurement

4.7.1 Wear rate

Wear rate was measured by diameter of the diamond wheel changed. Measuring of a diamond wheel diameter before (D_B) and after 150 cutting (D_A). The both diameter were measured by camera focus depth of cut on workpiece as shown in Figure 4.6. The wear rate can be calculation by using equation (4.1).

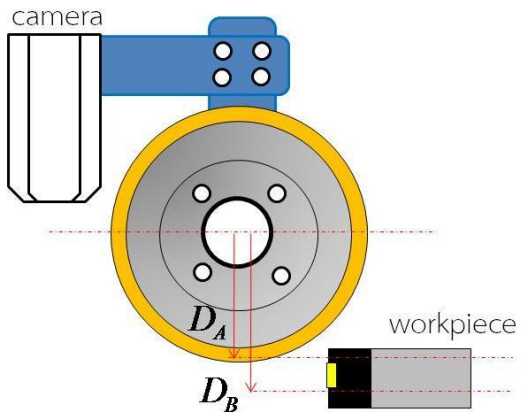

Figure 4.6 Wear rate measurement

$$Wear \quad rate \quad = \quad \frac{D_B - D_A(\mu m)}{150 \quad cuts} \tag{4.1}$$

Where

D_B is diamond wheel diameter before

D_A is diamond wheel diameter after

4.7.2 Chip size

The quality of the cut surface is measured in terms of the amount of chipping at edges. Measurement of the largest edge chipping was done on eight SEM images taken around cut surface. The representative value was obtained by averaging from eight largest edge chips of each images as shown in Figure 4.7 and calculated as equation (4.2).

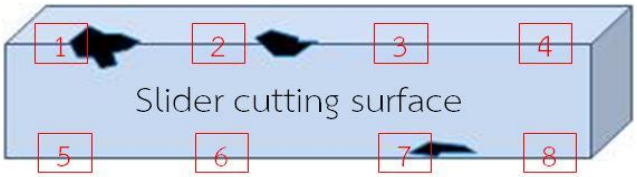

Figure 4.7 Chip size measurement (8 point of edge/slider)

$$Chip \quad size \quad average \quad = \quad \frac{C_1 + C_2 + \ldots + C_8}{8 \quad SEM \quad images} \tag{4.2}$$

Where C is largest edge chip of each SEM image.

4.7.3 Roughness

The surface roughness its own was another cut surface measurement. Roughness of center of the cut surface slider was measured by AFM in length 10 μm, as shown in Figure 4.8 and use arithmetic mean surface roughness (Ra) as equation (3.1) is indicator.

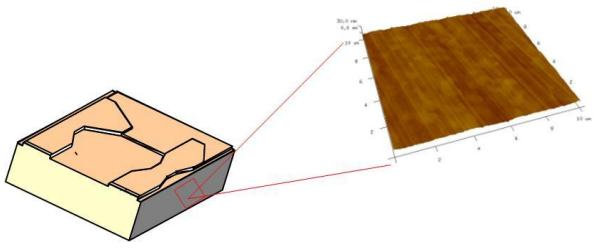

Figure 4.8 Roughness measurement

4.8 Experimental data analysis

Overview of experimental was shown in Figure 4.9.

4.8.1 Main effect test

In order to search for main effect on wear rate, chip size and roughness, experiments were set-up 2 factors at 2 levels and 5 replicates. There are 20 experiments totally.

4.8.2 DOE full factorial 2 parameters 3 levels

In order to search for main effect on wear rate, chip size and roughness, experiments were set-up 2 factors at 3 levels and 5 replicates. There are 45 experiments totally.

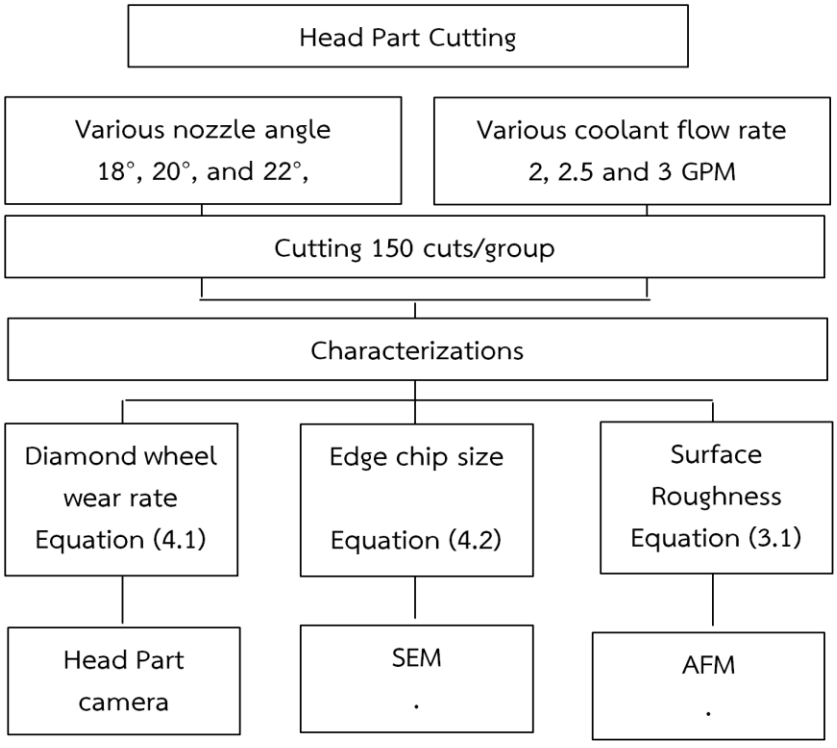

Figure 4.9 Flow chart of experiment

4.9 Optimization setup

For finding out optimized set point values of this experiment, the problem can be practically implemented in actual manufacturing as follows.

- Normalize data: The parameter values are normalized by following.

$$X_{normalized} = \frac{X_{actual} - MidPo\,\text{int}}{\frac{1}{2}Range} = \frac{X_{actaul} - \frac{1}{2}(X_{\max} + X_{\min})}{\frac{1}{2}(X_{\max} - X_{\min})} \tag{4.3}$$

  Hence, the factor levels are usually set at ±1. Assignment of coded values to qualitative factors is arbitrary, e.g. machines A and B can be assigned the coded values -1 and 1.

- Finding equation of nozzle angle and coolant flow rate related with wear rate, chip size and roughness
- Providing all equations to create objective function
- Setting up constraint equations
- Optimization analysis

CHAPTER 5

RESULTS AND DISCUSSION

The experimental results are discussed in three parts. The first part is showing effect of nozzle angle and coolant flow rate on wear rate, chip size and roughness. The second part is determining optimum values or setting values and model. The third part is extended wheel lift study by comparing wheel wear rate obtained by using original setting values and optimized setting values.

5.1 Analysis results of the main effect plot based on DOE method

5.1.1 Raw data

The raw data of nozzle angle and coolant flow rate at each 2 levels with 5 replications and results of wear rate, chip size and roughness are shown in Figure 5.1.

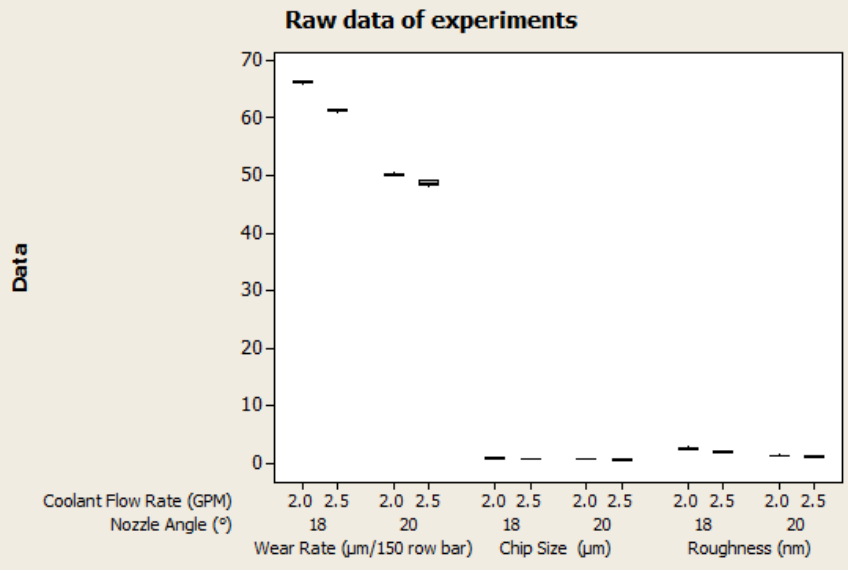

Figure 5.1 Raw data of experiments at 2 levels on 5 replicate

5.1.2 Main effect plot of wear rate

The result can be illustrated in main effect plot as shown in Figure 5.2 and 5.3. These plots are consist of low and high level of each factor as shown below.

1. Nozzle angle and coolant flow rate are significantly affected wear rate (p-value < 0.05)

2. From low to high level of nozzle angle rate, the wear rate is decreased trend from 64 to 49 μm/150 cut.

3. From low to high level of coolant flow rate, the wear rate is decreased trend from 58 to 55 μm/150 cut.

4. Nozzle angle is more sensitive to wear rate than coolant flow rate from 23% and 14% respectively.

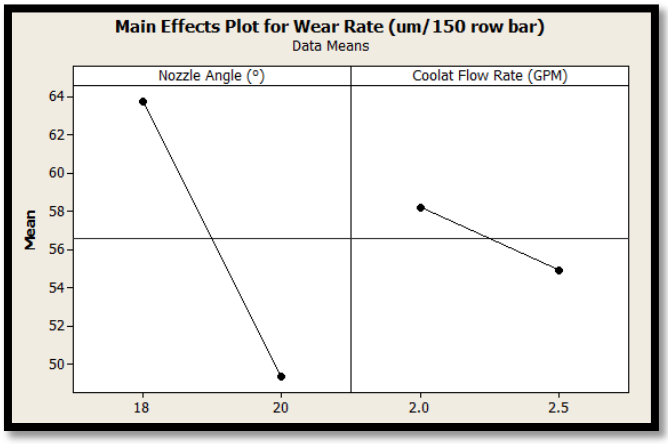

Figure 5.2 Main effect of nozzle angle and coolant flow rate to wear rate

Two-way ANOVA: Wear Rate (um/15 versus Nozzle Angle (°), Coolat Flow Rate

Source	DF	SS	MS	F	P
Nozzle Angle (°)	1	1027.03	1027.03	11751.94	0.000
Coolat Flow Rate (GPM)	1	52.81	52.81	604.31	0.000
Interaction	1	14.59	14.59	166.91	0.000
Error	16	1.40	0.09		
Total	19	1095.83			

S = 0.2956 R-Sq = 99.87% R-Sq(adj) = 99.85%

Figure 5.3 Two way anova wear rate vs. nozzle angle and coolant flow rate

5.1.3 Main effect plot of chip size

The result can be illustrated in main effect plot as shown in Figure 5.4 and 5.5. These plots consist of low and high level of each factor as shown below.

1. Nozzle angle and coolant flow rate significantly affected chip size (p-value < 0.05)

2. From low to high level of nozzle angle, the chip size is decreased trend from 0.90 to 0.70 μm.

3. From low to high level of coolant flow rate, the chip size is decreased trend from 0.82 to 0.77 μm.

4. Nozzle angle is more sensitive to chip size than coolant flow rate from 22% and 6% respectively.

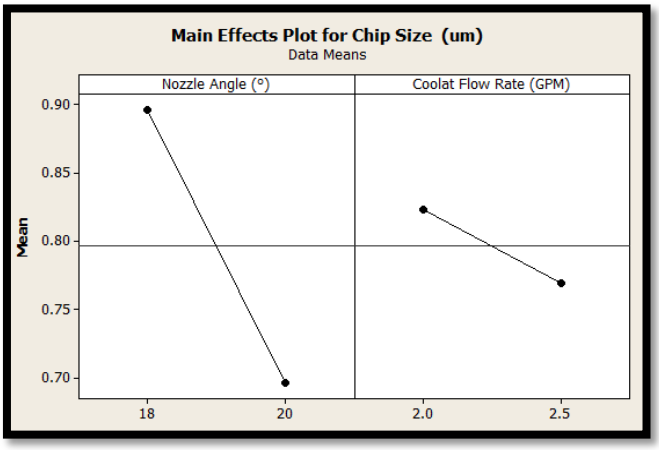

Figure 5.4 Main effect of nozzle angle and coolant flow rate to chip size

Two-way ANOVA: Chip Size (um) versus Nozzle Angle (°), Coolat Flow Rate (GPM)

Source	DF	SS	MS	F	P
Nozzle Angle (°)	1	0.197711	0.197711	193.40	0.000
Coolat Flow Rate (GPM)	1	0.014553	0.014553	14.24	0.002
Interaction	1	0.002370	0.002370	2.32	0.147
Error	16	0.016357	0.001022		
Total	19	0.230991			

S = 0.03197 R-Sq = 92.92% R-Sq(adj) = 91.59%

Figure 5.5 Two way anova chip size vs. nozzle angle and coolant flow rate

5.1.4 Main effect plot of roughness

The result can be illustrated in main effect plot as shown in Figure 5.6 and 5.7. These plots were consist of low and high level of each factor. From that were shown

1. Nozzle angle and coolant flow rate significantly affected roughness (p-value < 0.05)

2. From low to high level of nozzle angle, the roughness is decreased trend from 2.3 to 1.3 nm.

3. From low to high level of coolant flow rate, the chip size is decreased trend from 2.0 to 1.6 nm.

4. Nozzle angle is more sensitive to roughness than coolant flow rate from 43% and 20% respectively.

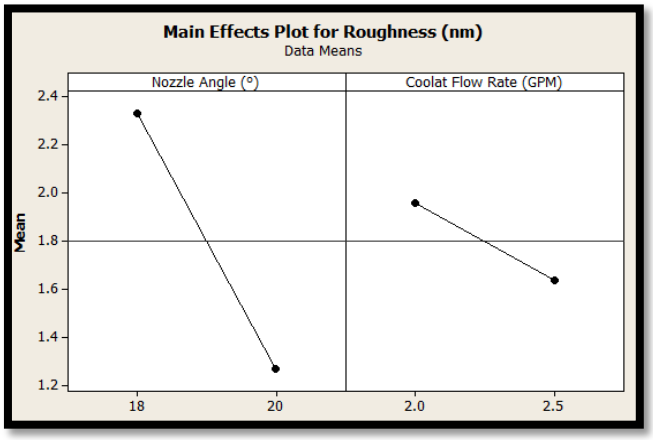

Figure 5.6 Main effect of nozzle angle and coolant flow rate to roughness

Two-way ANOVA: Roughness (nm) versus Nozzle Angle (°), Coolat Flow Rate (GPM)

Source	DF	SS	MS	F	P
Nozzle Angle (°)	1	5.618	5.61800	218.17	0.000
Coolat Flow Rate (GPM)	1	0.512	0.51200	19.88	0.000
Interaction	1	0.098	0.09800	3.81	0.069
Error	16	0.412	0.02575		
Total	19	6.640			

S = 0.1605 R-Sq = 93.80% R-Sq(adj) = 92.63%

Figure 5.7 Two way anova roughness vs. nozzle angle and coolant flow rate

5.2 Analysis of optimization

5.2.1 Raw data

Due to main effect testing, trend of wear rate, chip size and roughness can be reduced further and highly increased another level of the angle and flow rate. This experiment is 2 factors, 3 levels and 5 replications as condition as shown in Figure 5.8.

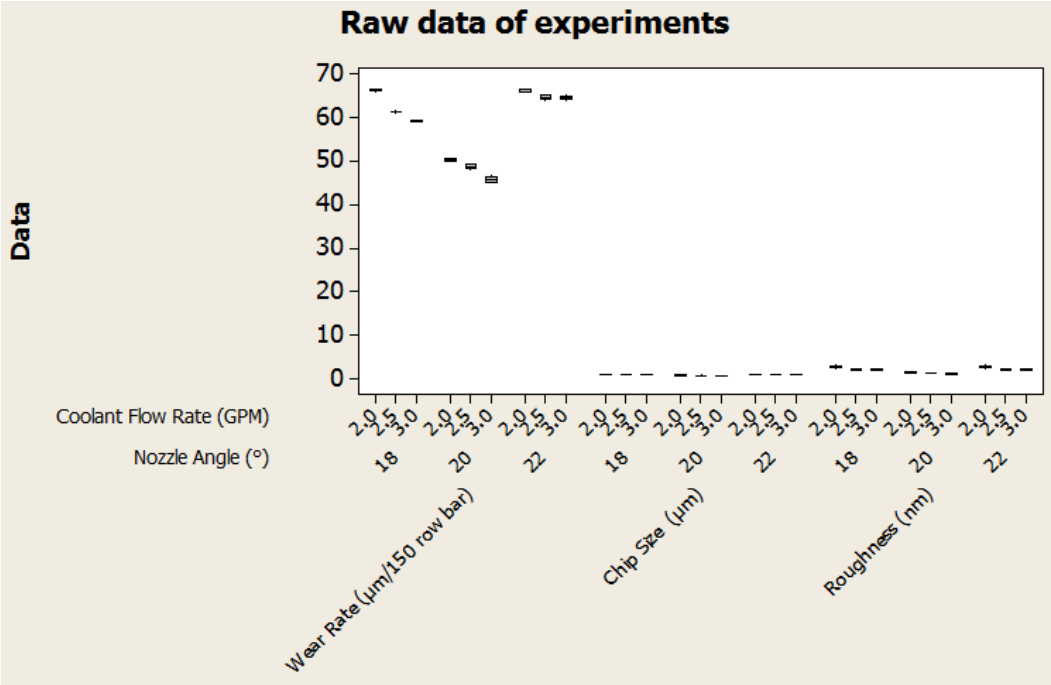

Figure 5.8 Raw data of experiments at 3 levels on 5 replicate

5.2.2 Normalized data

Due to the different data and magnitudes levels, their data will be normalized as explained in equation (4.1). After that, these data will be operated in RSM to get the format of nozzle angle, coolant flow rate, wear rate, chip size and roughness. The normalized data obtained as shown in Figure 5.9.

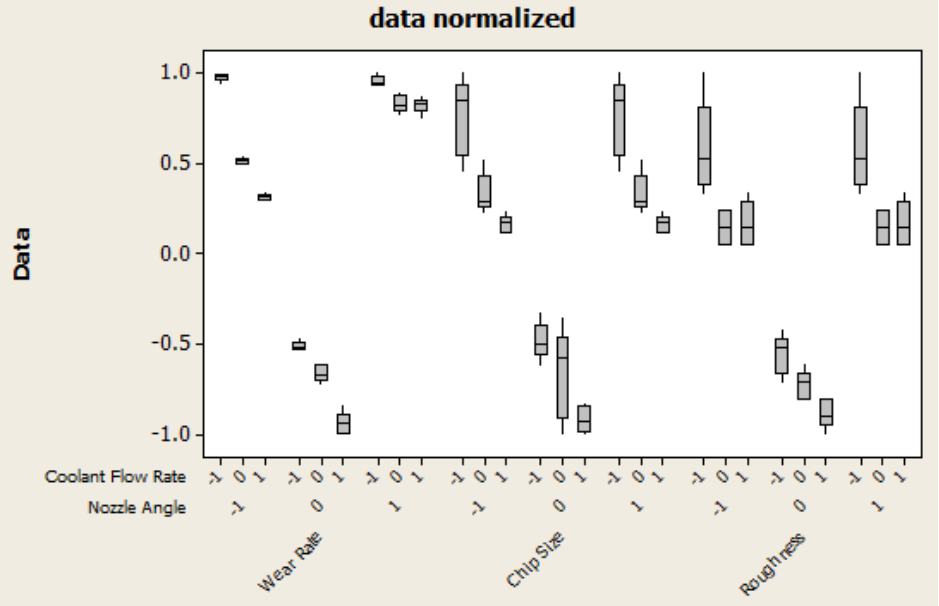

Figure 5.9 Raw data of data normalized

5.2.3 Response surface regression

5.2.3.1 Analysis of response surface regression of normalized wear rate with normalized nozzle angle and normalized coolant flow rate by an alpha (α) level of 0.05 was employed to determine the statistical significance of all analyses. The final quadratic model for each response in terms of coded levels is shown equation (5.1) which represents the final quadratic model for the normalized wear rate by given nozzle angle and coolant flow rate are $\overline{X_1}$ and $\overline{X_2}$ respectively. These equations have only statistically significant terms containing the lowest *P* value or ≤ 0.05 and eliminate these non-significant terms from the response equations as shown in Figure 5.10.

Response Surface Regression: Normalized W versus Nrmalized No, Normalized C

The analysis was done using uncoded units.

Estimated Regression Coefficients for Normalized Wear Rate

Term	Coef	SE Coef	T	P
Constant	-0.73410	0.018202	-40.332	0.000
Nrmalized Nozzle Angle	0.13247	0.009969	13.287	0.000
Normalized Coolant Flow Rate	-0.20359	0.009969	-20.422	0.000
Nrmalized Nozzle Angle* Nrmalized Nozzle Angle	1.43916	0.017268	83.345	0.000
Normalized Coolant Flow Rate* Normalized Coolant Flow Rate	0.04046	0.017268	2.343	0.024
Nrmalized Nozzle Angle* Normalized Coolant Flow Rate	0.13113	0.012210	10.740	0.000

S = 0.0546046 PRESS = 0.150594
R-Sq = 99.49% R-Sq(pred) = 99.34% R-Sq(adj) = 99.43%

Figure 5.10 Respond surface regression normalized wear rate

The predicted equation of normalized wear rate is

$$\overline{F}_{Wear(\overline{X}_1,\overline{X}_2)} = -0.73410 + 0.13247\overline{X}_1 - 0.20359\overline{X}_2 + 1.43916\overline{X}_1^2 + 0.04046\overline{X}_2^2 + 0.13113\overline{X}_1\overline{X}_2 \quad (5.1)$$

5.2.3.2 Analysis of response surface regression of normalized edge chip with normalized nozzle angle and normalized coolant flow rate by an alpha (α) level of 0.05 was employed to determine the statistical significance of all analyses. The final quadratic model for each response in terms of coded levels is shown equation (5.2) which represents the final quadratic model for the normalized edge chip by given nozzle angle and coolant flow rate are $\overline{X_1}$ and $\overline{X_2}$ respectively. These equations have only statistically significant terms containing the lowest *P* value or ≤ 0.05 and eliminate these non-significant terms from the response equations as shown in Figure 5.11.

Response Surface Regression: Normalized C versus Nrmalized No, Normalized C

The analysis was done using uncoded units.

Estimated Regression Coefficients for Normalized Chip Size

Term	Coef	SE Coef	T	P
Constant	-0.74059	0.05068	-14.614	0.000
Nrmalized Nozzle Angle	0.00000	0.02776	0.000	1.000
Normalized Coolant Flow Rate	-0.27093	0.02776	-9.761	0.000
Nrmalized Nozzle Angle* Nrmalized Nozzle Angle	1.10922	0.04808	23.072	0.000
Normalized Coolant Flow Rate* Normalized Coolant Flow Rate	0.07500	0.04808	1.560	0.127
Nrmalized Nozzle Angle* Normalized Coolant Flow Rate	0.00000	0.03399	0.000	1.000

S = 0.152030 PRESS = 1.20490
R-Sq = 94.17% R-Sq(pred) = 92.21% R-Sq(adj) = 93.42%

Figure 5.11 Respond surface regression normalized chip size

The predicted equation of normalized chip size is

$$\overline{F}_{Chip(\overline{X}_1,\overline{X}_2)} = -0.74059 + 0.27093\overline{X}_2 + 1.10922\overline{X}_1\overline{X}_2 \quad (5.2)$$

5.2.3.3 Analysis of response surface regression of normalized roughness with normalized nozzle angle and normalized coolant flow rate by an alpha (α) level of 0.05 was employed to determine the statistical significance of all analyses. The final quadratic model for each response in terms of coded levels is shown equation (5.3) which represents the final quadratic model for the normalized roughness by given nozzle angle and coolant flow rate are $\overline{X_1}$ and $\overline{X_2}$ respectively. These equations have only statistically significant terms containing the lowest *P* value or ≤ 0.05 and eliminate these non-significant terms from the response equations as shown in Figure 5.12.

Response Surface Regression: Normalized R versus Nrmalized No, Normalized C

The analysis was done using uncoded units.

Estimated Regression Coefficients for Normalized Roughness

Term	Coef	SE Coef	T	P
Constant	-0.83069	0.05190	-16.007	0.000
Nrmalized Nozzle Angle	0.00000	0.02842	0.000	1.000
Normalized Coolant Flow Rate	-0.19365	0.02842	-6.813	0.000
Nrmalized Nozzle Angle* Nrmalized Nozzle Angle	1.02222	0.04923	20.763	0.000
Normalized Coolant Flow Rate* Normalized Coolant Flow Rate	0.15556	0.04923	3.160	0.003
Nrmalized Nozzle Angle* Normalized Coolant Flow Rate	-0.00000	0.03481	-0.000	1.000

S = 0.155689 PRESS = 1.30052
R-Sq = 92.59% R-Sq(pred) = 89.81% R-Sq(adj) = 91.64%

Figure 5.12 Respond surface regression normalized roughness

The predicted equation of normalized roughness is

$$\overline{F}_{Roughness(\overline{X}_1,\overline{X}_2)} = -0.83069 - 0.19365\overline{X}_2 + 1.02222\overline{X}_1^2 + 0.15556\overline{X}_2^2 \qquad (5.3)$$

5.2.4 Surface plot

5.2.4.1 Normalized wear rate as a function of normalized nozzle angle and coolant flow rate

The surface plot showed a relation of normalized wear rate basing on the equation model. The relation exposed that normalized nozzle angle is more sensitive than normalized coolant flow rate. In other words, normalized nozzle angle influenced both wear rate as the arrow along normalized nozzle angle axis and surface as the increased slope as shown in Figure 5.13.

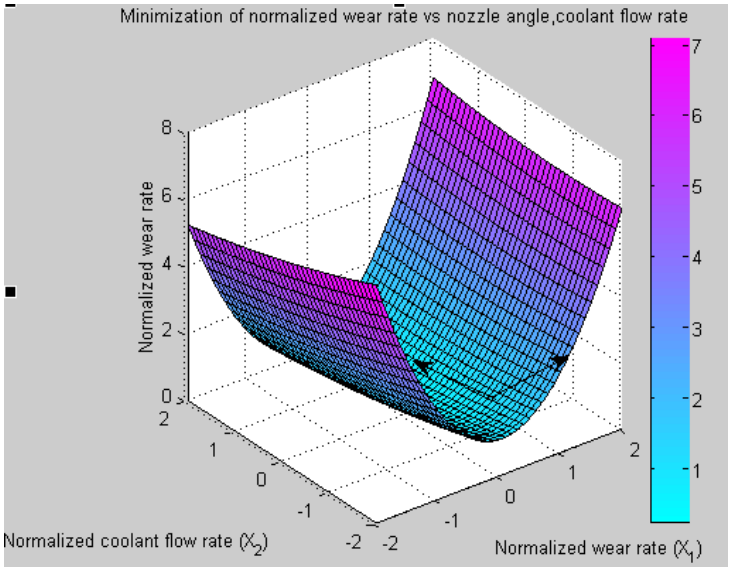

Figure 5.13 Surface plot of normalized wear rate

5.2.4.2 Normalized chip size as a function of normalized nozzle angle and coolant flow rate

The surface plot showed a relation of normalized chip size basing on equation model. The relation exposed that normalized coolant flow rate is more sensitive than normalized nozzle angle. In other words, normalized nozzle angle influenced both chip size as the arrow along normalized coolant flow rate axis and surface as the increased slope as shown in Figure 5.14.

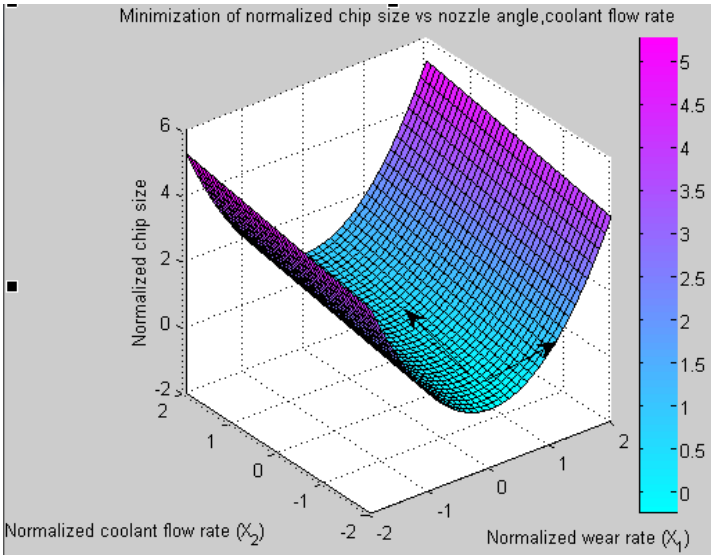

Figure 5.14 Surface plot of normalized chip size

5.2.4.3 Normalized wear roughness as a function of normalized nozzle angle and coolant flow rate

The surface plot showed a relation of normalized wear rate basing on the equation model. The relation exposed that normalized nozzle angle is more sensitive than normalized coolant flow rate. In other words, normalized coolant flow rate influenced both roughness as the arrow along normalized nozzle angle axis and surface as the increased slope as shown in Figure 5.15.

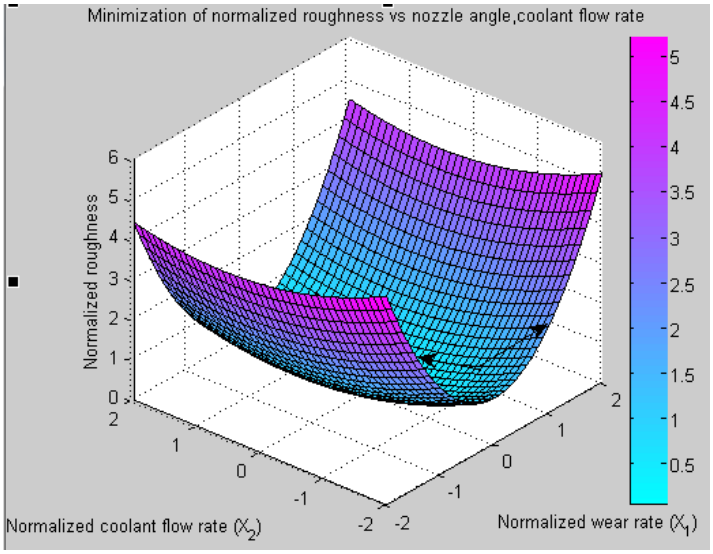

Figure 5.15 Surface plot of normalized roughness

5.3 Optimization

5.3.1 Definition of parameters in optimization study

Normalized nozzle angle	$[\overline{X_1}]$
Normalized coolant flow rate	$[\overline{X_2}]$
Normalized wear rate function	$[\overline{F}_{wear}]$
Normalized chip size function	$[\overline{F}_{chip}]$
Normalized roughness function	$[\overline{F}_{roughness}]$

5.3.2 Objective function $[\overline{F}_{obj}]$ used in this study is

$$\text{Minimize} \qquad \overline{F}_{obj} = W_1\overline{F}_{wear} + W_2\overline{F}_{chip} + W_3\overline{F}_{roughness} \tag{5.4}$$

W_1, W_2 and W_3 are weighting factors of $\overline{F}_{wear}$, $\overline{F}_{chip}$ and $\overline{F}_{roughness}$ respectively. In this study, $W_1 = 0.6$, $W_2 = 0.3$ and $W_3 = 0.1$.

Replacing (5.1), (5.2), (5.3) in (5.4)

Minimize $\overline{F}_{obj}$ = (0.6) ($\overline{F}_{wear}$) + (0.3) ($\overline{F}_{chip}$) + (0.1) ($\overline{F}_{roughness}$)

5.3.3 Identification of constraints

There are three constraints deriving from normalized wear rate, chip size and roughness which setup target values obtained from physical values are 42.29 μm/150 cuts, 0.62 μm and 0.95 nm respectively and convert to be normalized data from equation (4.3) are 1.25, 1.05 and 0.95 respectively, as follows.

$$1.25 - \overline{F}_{wear} \leq 0$$

$$1.05 - \overline{F}_{chip} \leq 0$$

$$0.95 - \overline{F}_{roughness} \leq 0$$

Also there are 2 boundary conditions for the design variables from physical values can be setup into constraints, nozzle angle since 16° until 24° and coolant flow rate since 1.5 until 3.5 GPM which both variable can be converted to normalized data from equation (4.3) since -2 until 2, as follows.

$$-2 \leq \overline{X_1} \leq 2$$

$$-2 \leq \overline{X_2} \leq 2,$$

Thus, the objective function and multivariable with inequality constraints problem are

$$\text{Minimize} \quad \overline{F}_{obj} = -0.74571 + 0.07982\overline{X}_1 - 0.06024\overline{X}_2 + 1.29848\overline{X}_1^2 + 0.179836\overline{X}_2^2 + 0.078678\overline{X}_1\overline{X}_2 \tag{5.5}$$

And inequality constraints are

$$\text{Subject to} \quad \begin{cases} -2 \le \overline{X_1} \le 2, & (5.6a) \\ -2 \le \overline{X_2} \le 2, & (5.6b) \\ 1.25 - \overline{F}_{wear} \le 0, & (5.6c) \\ 1.05 - \overline{F}_{chip} \le 0, & (5.6d) \\ 0.95 - \overline{F}_{roughness} \le 0, & (5.6e) \end{cases}$$

5.3.4 Optimization: Minimum setting of normalized nozzle angle and coolant flow rate by MATLAB

From equation (5.6a) to (5.6e), the minimum of normalized nozzle angle and coolant flow data was -0.14 and 1.4 respectively as shown in Figure 5.16. The data was obtained by find minimum of constrained nonlinear multivariable function (fmincon) of MATLAB.

```
Local minimum found that satisfies the constraints.

Optimization completed because the objective function is non-decreasing in
feasible directions, to within the default value of the function tolerance,
and constraints were satisfied to within the default value of the constraint tolerance.

<stopping criteria details>

Active inequalities (to within options.TolCon = 1e-006):
  lower      upper     ineqlin   ineqnonlin
                                     1

x =

   -0.1404    1.4385


fval =

   -0.4618
```

Figure 5.16 The optimum normalized nozzle angle and coolant flow rate obtained from MATLAB

5.3.4 Graphical of optimization

The optimum nozzle angle and coolant flow rate can be shown in graphical form as depicted as shown in Figure 5.17 as a plotted objective function and all referred constraint functions. The optimum setting points for normalized nozzle angle and normalized coolant flow rate in head part process are -0.14 (or 19.7°) and 1.43 (or 3.2 GPM) respectively. As the figure demonstrated: the objective function is solid line and three constraints are dot line arranging by size from thinner, regular and bulky represent of $\overline{F}_{wear}$ $\overline{F}_{chip}$ and $\overline{F}_{roughness}$ respectively.

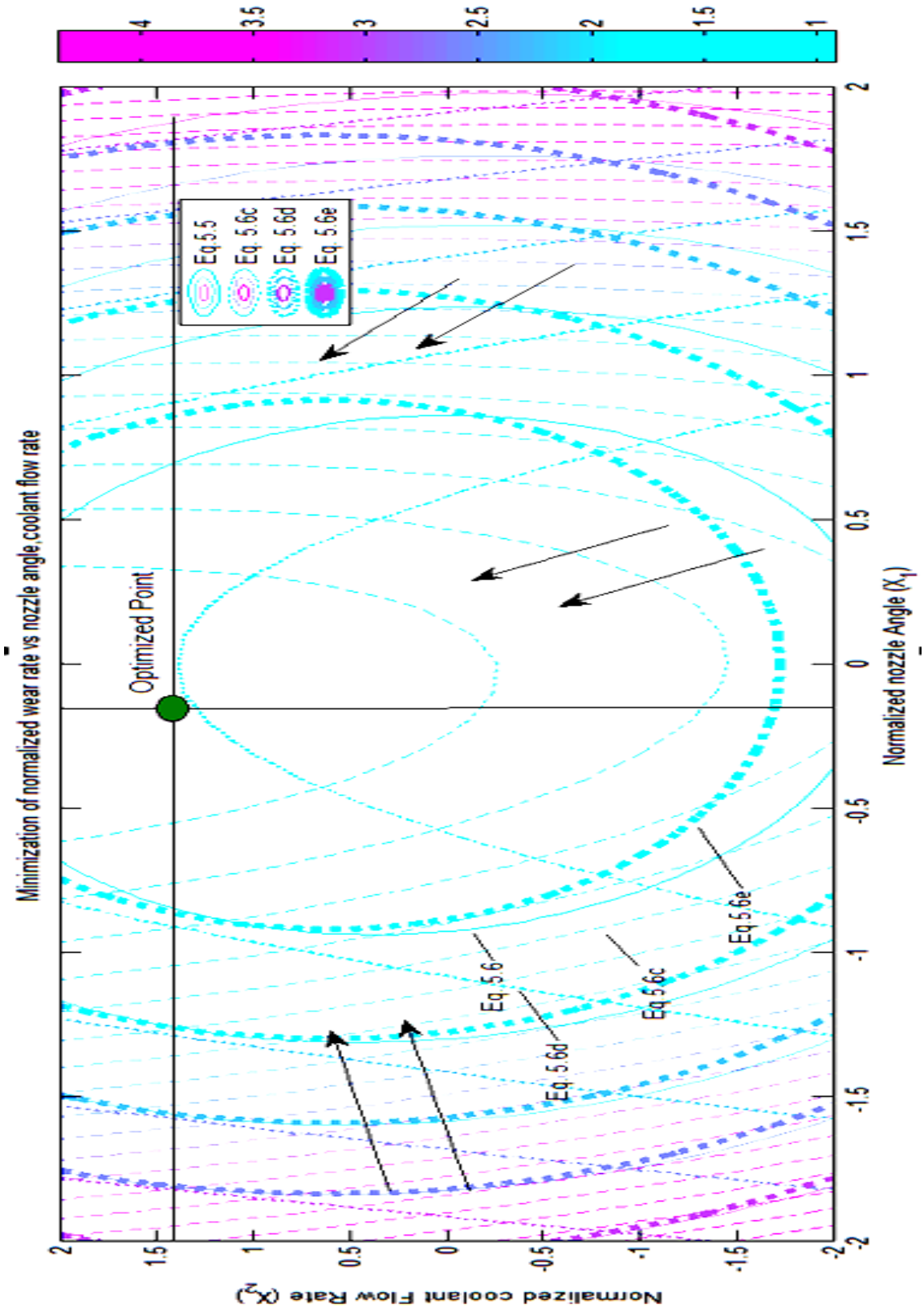

Figure 5.17 Graphical solutions to the minimization

5.4 Validation

Based on the prediction model, the wear rate, chip size, roughness can be computed from equation (4.1), (5.1), (5.2) and (5.3). The model can calculate cost of each varying variable for prediction and find desirable values as shown in Table 5.1. For example, at optimum in green colored row, the nozzle is 19.7°, coolant flow rate is 3.2 GPM. According to mentioned model, computed wear rate is 46.09 μm/150 cuts, chip size is 0.72 μm and roughness is 1.04 nm. Despite the error of nozzle angle adjustment for +/- 1° or 2°, nozzle angle has considerable effect on wear rate and cost loss. There are also some differences in term of wear rate related to cost as table below, comparing between max and min of wear rate (the nozzle angle at 22° and 20°) that resulted in lowest cost at optimum.

Table 5.1 Example comparing of prediction of wear rate, chip size and roughness

Point	Normalized values		Prediction				
	Nozzle angle	Coolant flow rate	Nozzle angle (°)	Coolant flow rate (GPM)	Wear rate (μm)	Chip size (μm)	Roughness (nm)
+	1	1	22	3	64.41	0.91	2.11
	0.5	1	21	3	51.38	0.77	1.31
Optimum	0	1	20	3	46.09	0.72	1.04
-	-0.5	1	18	3	48.54	0.77	1.31
	-1	1	17	3	58.73	0.91	2.11

According to historical wear rate of diamond wheel and the wear rate after nozzle at 20° and coolant flow rate at 3 GPM was implemented, the wear rate was reduced from 17 µm/150 cuts to 15 µm/150 cuts as shown in Figure 5.18 or 11.8% of cost per quarter. Also in-term of cutting quality surface, the chip size and the roughness were reduced from 0.9 µm to 0.6 µm and 2 nm to 1 nm respectively as shown in Figure 5.19.

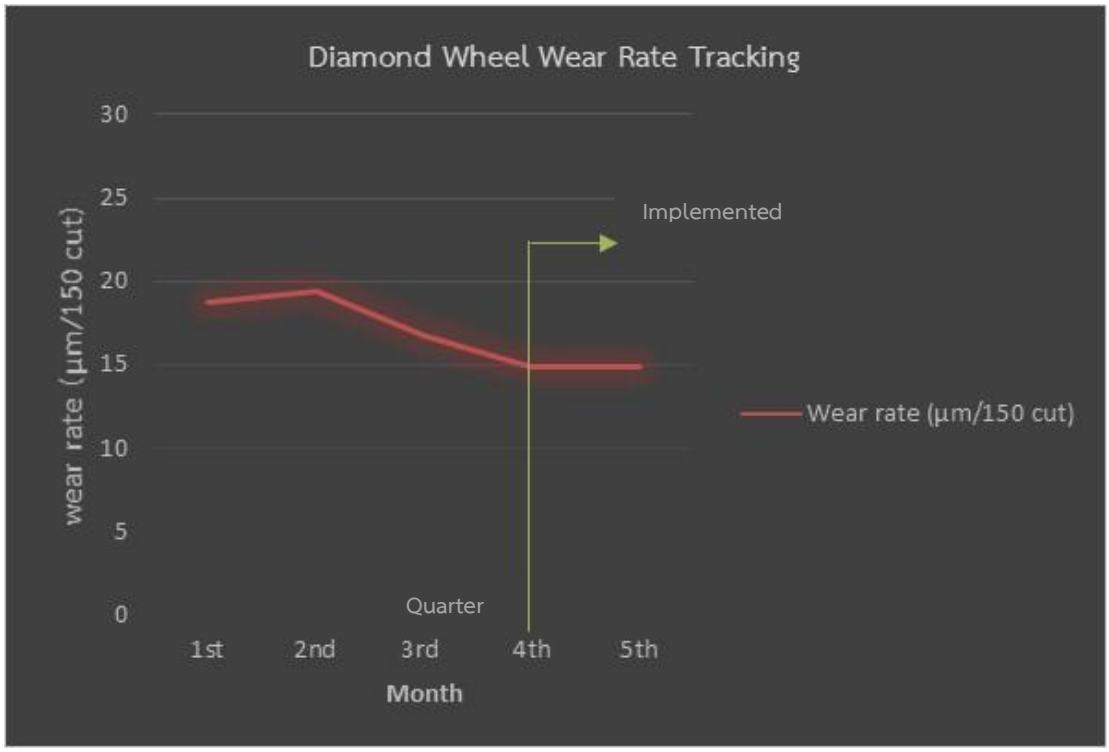

Figure 5.18 Diamond wheel wear rate tracking

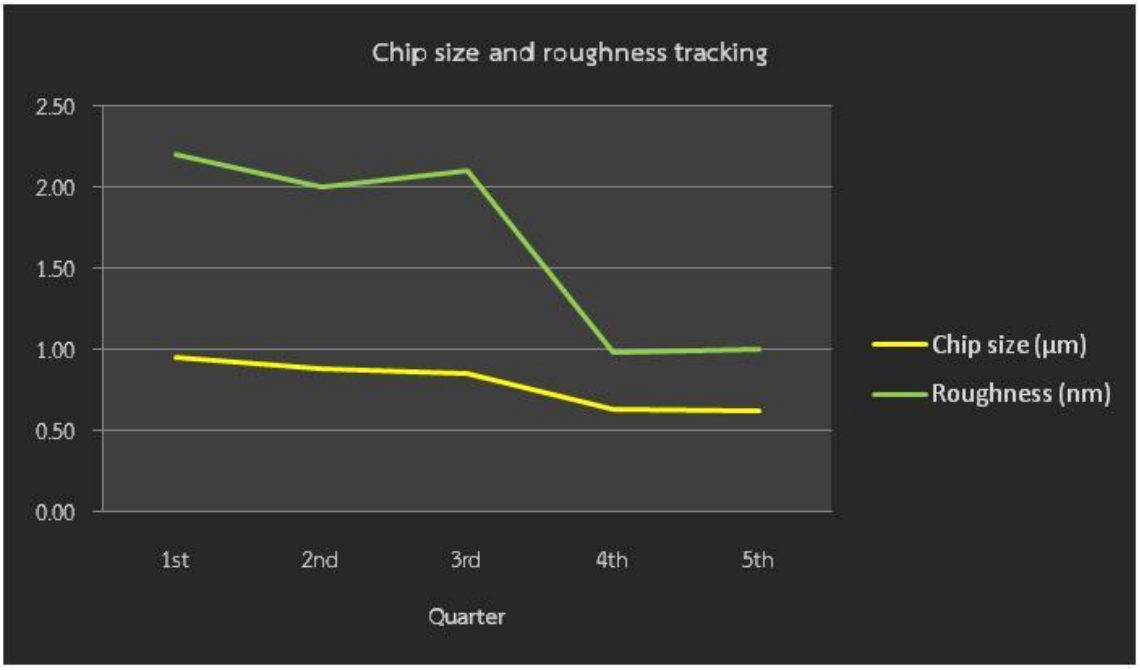

Figure 5.19 Chip size and roughness tracking

CHAPTER 6

CONCLUSION AND SUGGESTION

6.1 Conclusion

Among numerous cut-off grinding parameters operation, the coolant nozzle angle and the flow rate are two important parameters affecting cut surface quality and wear rate of diamond grinding wheel. Little adjustments of coolant nozzle angle has greatly effect on wheel wear rate and edge chipping amout of the cut surface. The coolant flow rate of 3.2 GPM is sufficient for the cut-off grinding operation as the nozzle angle optimized at 19.7°. According to research results, the conclusion can be made as follows.

6.1.1 The nozzle angle and coolant flow rate directly affects increasing wear rate ,chip size and roughness on cutting surface of diamond wheel.

6.1.2 The nozzle angle at 19.7° and coolant flow rate at 3.2 GPM are the optimum set points when the objective function is

Minimize $\overline{F}_{obj} = -0.74571 + 0.07982\overline{X}_1 - 0.06024\overline{X}_2 + 1.29848\overline{X}_1^2 + 0.179836\overline{X}_2^2 + 0.078678\overline{X}_1\overline{X}_2$

6.1.3 According to optimum set points, the implementation in actual production, the diamond wheel wear rate is remained 15 μm/150 cuts per quarter. If calculated per slider, the cost saving is reduced by 11.8%.

6.2 Suggestion

6.2.1 In accordance with literature reviews, depth of cut, feed rate of diamond wheel also affect to wear rate and cutting surface. Thus these parameters can be taken to study for future research.

6.2.2 Coolant flow rate can be adjusted in more diversified range.

6.2.3 Wear rate can be adjusted by changing coolant nozzle shape.

6.2.4 Chip size can be more accurately characterized with 3D visualization.

REFERENCES

[1] S. Ebbrell, H.H. Woolley, Y.D. Tridimas, D.R. Allanson, W.B. Rowe," Cutting Fluid Can Be Overcome Boundary Layer", School of Engineering, Liverpool John Moores University, Liverpool L3 3AF, UK, 1999

[2] Hans H. Gatzen, Jeihad Zeadan, "Investigation on The Coolant Supply in Precision Dicing Institute for Microtechnology", Hanover University, Germany

[3] Hoh Huey Jiun, Ibrahim Ahmad, Member, IEEE, Azman Jalar, and Ghazali Omar, Member, IEEE, "Effect of Laminated Wafer Toward Dicing Process and Alternative Double Pass Sawing Method to Reduce Chipping", 2006

[4] W.Li, Y. Wang, Shouhong Fan, Jinfu Xu, PR China, "Wear of Diamond Grinding Wheels and Material Removal Rate of Silicon Nitrides under Different Machining Conditions", 2006

[5] Czenkusch, C., to be published soon, Technologie und Prozemoelle beim Rundschleifen, Dr.-Ing Diss., Fakultat fur Maschinenwesen, Universitat Hannover.

[6] Weinert, K.; Buschka, M.; Johlen, G.; Schleifen mit Graphit als Schmierstoff, VDI-Z 140/1/2:46-49, 1998

[7] Loan D. Marinescu, "Technology of Abrasive Machining Process", Copyright © 2004 by William Andrew, Inc. 265-268.

[8] Nakayama, K., Elastic Deformation of Contact Zone in Grinding, Bull. Jpn. Soc. Precision Eng., 5(4):93-98, 1972

[9] Brinksmeier, E.; Heinzel, C., Grundlagen und heutige Anwendung von Kühlschmierstoffen, Seminar: Deutsches Indusrieforum fur Technologie, 1996

[10] Kleijnen, J.P.C., ”Senstivity analysis and optimization in simulation: design of experiments and case studies”, Proceeding of 1995 IEEE Simulation conference. Dec,1995, pp. 133-140

[11] Brady, N., “The response surface methodology”, A thesis presented to Indiana of South Bend, Indiana, USA, 2007.

[12] Jabir, S., “Introduction to Optimum Design”, The University of IOWA, Academic press California, 2004.

[13] Bhatti, M, “Practical Optimization Method with Mathematica Applications”, Springer-Verlag, New York, 1998.

APPENDIX A

PUBLICATION

This work has been published and presented in the 19th International Annual Symposium on Computational Science and Engineering at Ubon Ratchathani University, Ubon Ratchathani, Thailand, on June 17-19, 2015.

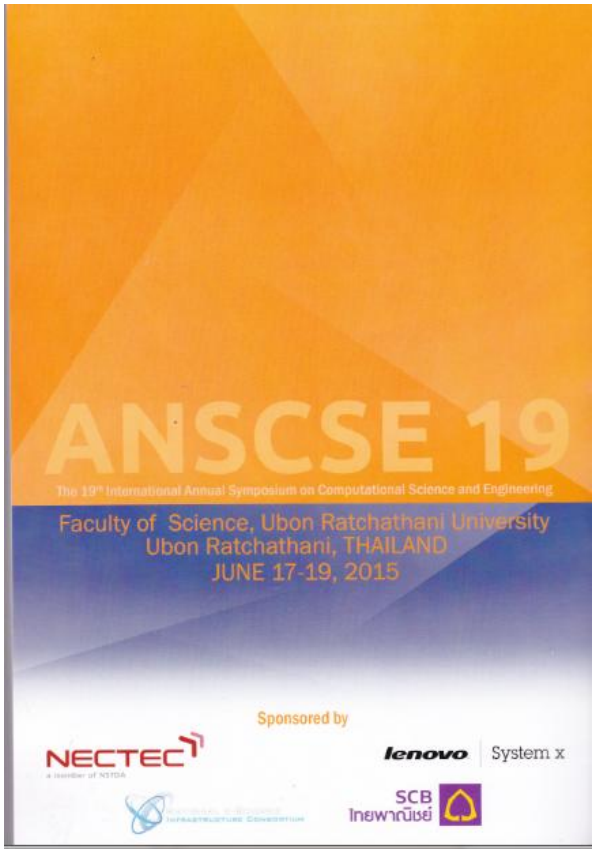

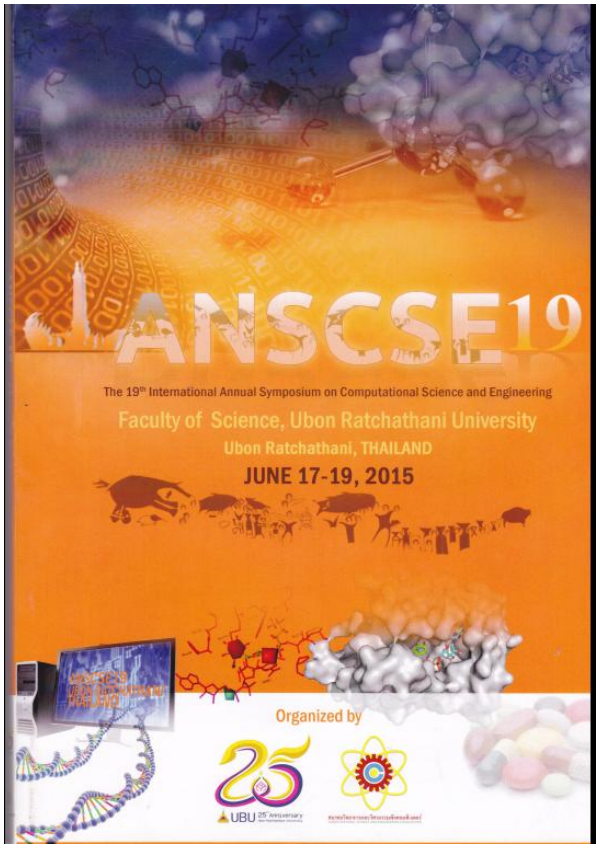

Computational Mathematics, Computational Fluid Dynamics and Solid Mechanics, High Performance Computing and Grid computing, Computer Science and Engineering
June 18, 2015 **Room SC248**

Time	Speaker	Name	Title
Chair: Dr. Supakit Prueksaaroon			
09.00-09.15	O-CSE12	Auttarat Nawikavatan	Optimal PID Controller Design for Three-Phase Induction Motor Speed Control by Intensified Current Search
09.30-09.45	O-CSE13	Komate Amphawan	Mining top-k frequent-regular patterns based on user-given length constraints
09.45-10.00	O-CSE14	Boonruang Wangsilabatra	Bi-Objective Optimization for State-Space Model Identification of BLDC Motor by Intensified Current Search
10.00-10.15	O-CSE15	Kachamart Manokruang	Optimum Study Slider Bar Dicing Parameters for Minimizing Diamond Wheel Wear
10.15-10.30	O-CSE16	Chookiat Kiree	Application of Particle Swarm Optimization to Identify Model Parameters of BLDC Motor
10.20-10.35	**Coffee break**		
Chair: Dr.Jirutchaya Jaisaardsuetrong			
10.35-10.50	O-CFD01	Poompong Yuthanasirikul	Comparison between Weakly Compressible and Implicit Incompressible Smoothed Particle Hydrodynamics
10.50-11.05	O-CFD02	Nissaya Chuathong	Numerical solutions of 2D nonlinear PDEs using The Kansa's meshless method and the search for optimal radial basis function
11.05-11.20	O-CFD03	Kritsidej Chanthawara	Inverse Multiquadric RBF in the Dual Reciprocity Boundary Element Method (DRBEM) for Coupled 2D Burgers' Equations at high Reynolds numbers
11.20-11.35	O-CFD04	Wachirapond Pempoonsinsap	The Monsoon Precipitation Intensity and Climate Anomaly of China and Thailand
11.35-11.50	O-CFD05	Pongjet Promvonge	Numerical Investigation of Turbulent Flow and Heat Transfer in Circular and Oblique-Elliptical Section Tube
11.50-12.05	O-CFD06	Sombat Tamna	Numerical Study on Turbulent Flow and Heat Transfer in Square Channel with 30° Delta-winglets
12.00-13.00	**Lunch time**		

UBU 25th Anniversary

ANSCSE 19

The 19th International Annual Symposium on Computational Science and Engineering

Certificate of Appreciation for Your Contribution as a Presenter at

The 19th International Annual Symposium on Computational Science and Engineering

JUNE 17-19, 2015
Faculty of Science, Ubon Ratchathani University
Ubon Ratchathani, Thailand

Presented to

Katchamart Manokruang

Associate Professor Dr. Utith Inprasit
Dean of Faculty of Science,
Ubon Ratchathani University

สมาคมวิทยาการและวิศวกรรมเชิงคอมพิวเตอร์
COMPUTATIONAL SCIENCE AND ENGINEERING ASSOCIATION

Assistant Professor Dr. Putchong Uthayopas
President of Computational Science and
Engineering Society, Thailand

Optimum Study Slider Bar Dicing Parameters for Minimizing Diamond Wheel Wear

K. Manokruang[1,A] and M. Pimsarn [2]

[1] *College of Data Storage Innovation, King Mongkut's Institute of Technology Ladkrabang, Bangkok 10520, Thailand*

[2] *1Faculty of Engineering, King Mongkut's Institute of Technology Ladkrabang, Bangkok 10520, Thailand*

[A]**E-mail**: Katchamart.manokruang@wdc.com; **Tel.** +66846426535

ABSTRACT

The Hard Disk Drive (HDD) industry is highly competitive. Cost reduction in manufacturing is a very important to remain competitive. This research focuses on the production of a HDD slider. One of the process steps to make a slider is to cut the slider bar with a diamond wheel. This paper presents the study by means of experiment to see the effects of the variables, nozzle angle and coolant flow rate, on the wear of diamond blades, slider chip size and roughness of cutting surface. Design of Experiment (DOE) was used to record the effects of the two variables. The results of the DOEs were used to build a relationship and response surface method (RSM). From the optimization analysis, the most appropriate coolant nozzle angle nozzle is 19.7° and the coolant flow rate is 3.2 gallons per minute (GPM). Thus, this leads to the cost saving of diamond wheel, US$ 100,000 per quarter.

Keywords: dicing diamond wheel, precision grinding, hard disk drive, slider bar

1. INTRODUCTION

The slider is one of the many components in the hard disk drive assembly. It is basically a head or device used to read and write data from and onto the disk. The slider is made in the slider fabrication process, and dicing is one of the processes involved. The dicing process requires a cutting tool as an abrasive material, known as the diamond wheel, for cutting the slider from the wafer. Because of their high usage rate and expense, diamond wheels are the major cost factor in the dicing process. Extending the life of the diamond wheel by reducing the wear rate is an effective pursuit for cost reduction in the dicing process.

2. THEORY AND RELATED WORKS

In an effort to reduce wheel wear rate, a coolant is delivered in a correct direction and area onto the diamond wheel where it interacts with the slider part (cutting area or heat affected zone) to function as a lubricant and prevent heat transfer. Efficient slicing will reduce the wear rate. On the other hand, incorrect direction of the coolant will decrease the heat transfer [1]. High coolant volume by simple feed shoe to the cutting zone is effective at low wheel speed but ineffective at high wheel speed [2]. Using a nozzle jet could be effective by fluid laminar flow. The jet has no air and achieves high fluid velocity at the cutting zone. The benefit is reaching the cutting zone and helping to clean the grinding swarf [3]. Nozzle position was shown to affect the fluid volume that actually reaches the cutting zone. The result was shown to improve work piece quality in terms of surface roughness [4].

3. EXPERIMENTAL or COMPUTATIONAL DETAILS

A schematic drawing of cut-off grinding of the slider bar, using an SD8000 diamond wheel, and the coolant delivery system are shown in Figure 1. The values of the coolant nozzle angle and flow rate in the experiment are shown in Table 1. There are five repeats for each condition. DOE was used to record the effects of the two variables, due to multi variables unit transfers to data normalized as Eq. (1). Then used Analysis of variance (ANOVA) with an

alpha (α) level of 0.05 was employed to determine the statistical significance of all analyses and got the final quadratic model for each response which can be build the relationship on response surface method (RSM) for optimization to find the setting value.

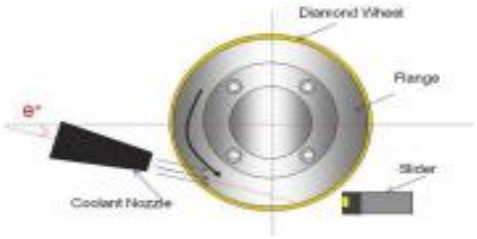

Figure 1 Schematic of coolant delivery from nozzle jet passed through the wheel and work piece while cutting

Variables	High	Mid	Low
Nozzle Angle (°)	18	20	22
Coolant Flow Rate (GPM)	2	2.5	3

Table 1 Experiment condition

$$X_{normalized} = \frac{X_{actual} - MidPoint}{\frac{1}{2}Range} = \frac{X_{actual} - \frac{1}{2}(X_{max} + X_{min})}{\frac{1}{2}(X_{max} - X_{min})} \quad (1)$$

Parametric Study

There are three key parameters selected in order to study the effect of the nozzle angle and coolant flow rate in the slider cutting process.

1.) Blade Wear Rate: The wear rate was measured by comparing the outside diameter of the blade before and after 150 cuts.

2.) Slider Edge Chipping: Measurement of the largest edge chipping (Figure 2) was done on eight SEM images taken around the cut surface. The representative value is obtained by averaging the nine largest edge chips from each of the nine images.

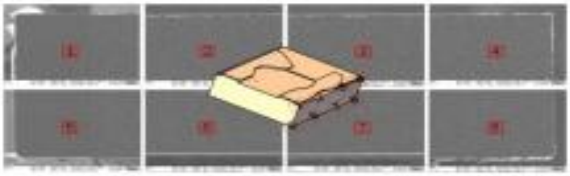

Figure 2 only the largest edge chip on the cut surface is measured from each SEM image of the sidewall of the slider

3.) Roughness: Roughness of the center of the cut surface was measured by AFM as Figure 3.

Figur 3 Roughness and sampling

4. RESULTS AND DISCUSSION

Main effect plot: The variables of nozzle angle and coolant flow rate have significant effect to wear rates of the diamond wheel after 150 cuts, chip size and roughness shown in Figure 4. The three both parameters are reduced where increased nozzle angle and coolant flow rate.

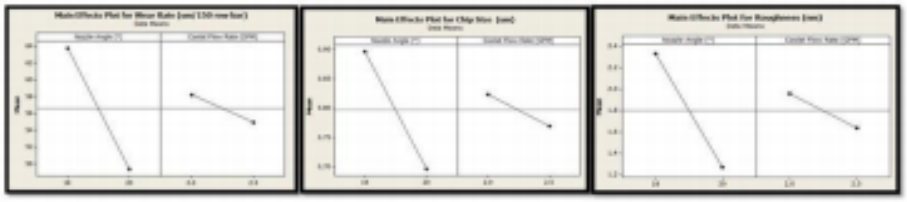

Figure 4 Main effect plots by parameters

Optimization: After the real data to normalized from Eq. (1). Then analysis of Response Surface Regression of normalized of wear rate, chip size and roughness with normalized nozzle angle and normalized coolant flow rate by an alpha (α) level of 0.05 was defined to determine the statistical significance terms. Thus, will be equation have only statistically significant terms containing which eliminated all non-significant terms and obtained equations as follow.

$$F_{wear} = -0.7310 + 0.13247X_1 - 0.20359X_2 + 1.43916X_1^2 + 0.04046X_2^2 + 0.13113X_1X_2 \quad (2)$$

$$F_{chip} = -0.74059 + 0.27093X_2 + 1.10922X_1X_2 \quad (3)$$

$$F_{roughness} = -0.83069 - 0.19365X_2 + 1.0222X_1^2 + 0.15556X_2^2 \quad (4)$$

Where X_1 and X_2 are represent the nozzle angle and the coolant flow rate. The objective function (F_{obj}) can be expressed and also weighting score in term as

$$F_{obj} = W_1F_{wear} + W_2F_{chip} + W_3F_{roughness} \quad (5)$$

Thus, from Eq. (5) replaced by (2), (3) and (4) and given W_1, W_2 and W_3 are 0.6, 0.3 and 0.1 the objective function as below

$$\text{Min } F_{obj} = -0.74571+0.07982X_1-0.0602X_2+1.2984X_1^2+0.179836X_2^2+0.07867X_1X_2 \quad (6)$$

And multivariable with inequality constraints is

$$\text{Subject to} \quad \begin{cases} -1 \le X_1 \le 1, \\ -1 \le X_2 \le 1, \\ 1.25 - \bar{F}_{wear} \le 0, \\ 1.05 - \bar{F}_{chip} \le 0, \\ 0.95 - \bar{F}_{roughness} \le 0, \end{cases} \tag{7}$$

Given $\bar{F}_{wear}$, $\bar{F}_{chip}$ and $\bar{F}_{roughness}$ are Eq. (2),(3) and (4) respectively.

The graphical is plotted from Eq. (6) and (7) can be found graphical as Figure 5, an objective function and all constraint function are plotted. Thus, the minimum points for normalized nozzle angle and normalized coolant flow rate in Head Part process are -0.14 (or 19.7°) and 1.43 (or 3.2 GPM), respectively. As the figure are shown that the objective function is solid line and three constraints are dot line arranging by size from thinner, regular and bulky represent of $\bar{F}_{wear}$, $\bar{F}_{chip}$ and $\bar{F}_{roughness}$ respectively. The minimum point or setting values are computed with Eq. (1), (2), (3), (4) and given wear rate, chip size and roughness are 46.09 µm, 0.72 µm, and 1.04 nm, respectively.

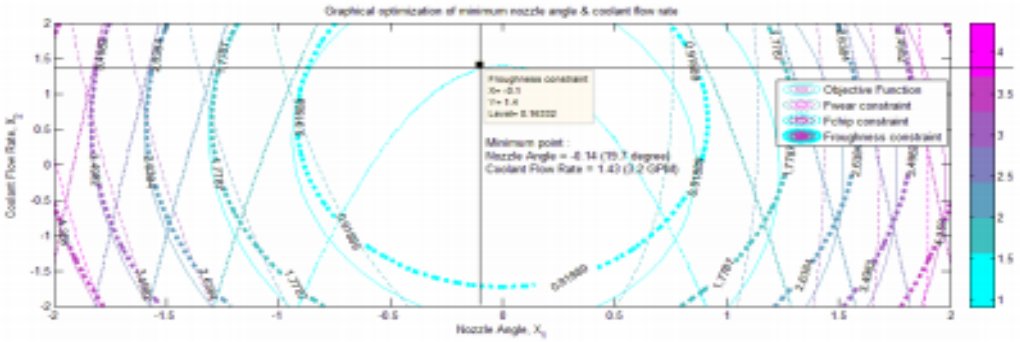

Figure 5 Graphical optimization of minimum nozzle and coolant flow rate

Economic study: Based on the prediction model that can do compute the wear rate, chip size, roughness and get cost each variable is varied as for prediction and find desirable values. For example, at optimum the nozzle is 19.7° and coolant flow rate is 3.2 GPM the model is used compute wear rate is 45.98 µm/150 cuts, chip size is 0.72 µm, roughness is 1.04 nm and total cost is US$ 202,237, which comparison with max and min of the nozzle angle (20.4° and 19.4°) the optimum shown cost is cheaper.

5. CONCLUSION

Among numerous cut-off grinding operating parameters, the coolant nozzle angle and the flow rate are two important parameters which affect the cut surface quality and the wear rate of the diamond grinding wheel. According to this research results, the conclusion can be made as follow.

1. The nozzle angle and coolant flow rate have affected to wear rate on diamond wheel, chip size and roughness on cutting surface. As the nozzle angle is increased the wear rate, chip size and roughness are decreased. As the coolant flow rate is increased the wear rate, chip size and roughness are decreased.

2. The nozzle angle at 19.7° and coolant flow rate at 3.2 GPM is optimum and obtained the model equation as per below.

$$\text{Min } F_{obj} = -0.74571+0.07982X_1-0.0602X_2+1.2984X^2_1+0.179836X^2_2+0.07867X_1X_2$$

3. From optimum set points, after implemented in actual production, the cost saving of diamond wheel is US$ 100,000 per quarter.

REFERENCES

[1] S. Ebbrell, H.H. Woolley, Y.D. Tridimas, D.R. Allanson, W.B. Rowe," Cutting Fluid Can Be Overcome Boundary Layer", School of Engineering, Liverpool John Moores University, Liverpool L3 3AF, UK, 1999

[2] Hans H. Gatzen, Jeihad Zeadan, "Investigation on The Coolant Supply in Precision Dicing Institute for Microtechnology", Hanover University, Germany

[3] Hoh Huey Jiun, Ibrahim Ahmad, Member, IEEE, Azman Jalar, and Ghazali Omar, Member, IEEE, "Effect of Laminated Wafer Toward Dicing Process and Alternative Double Pass Sawing Method to Reduce Chipping", 2006

[4] W.Li, Y. Wang, Shouhong Fan, Jinfu Xu, PR China, "Wear of Diamond Grinding Wheels and Material Removal Rate of Silicon Nitrides under Different Machining Conditions", 2006

ACKNOWLEDGMENTS

This work was supported by Western Digital (Thailand) and DSTAR (KMITL) and the authors would like to thank Asst. Dr. Monsak Pimsarn for his valuable comments and suggestions to improve the manuscript.

APPENDIX B

MATLAB CODE

1. Define the objective function

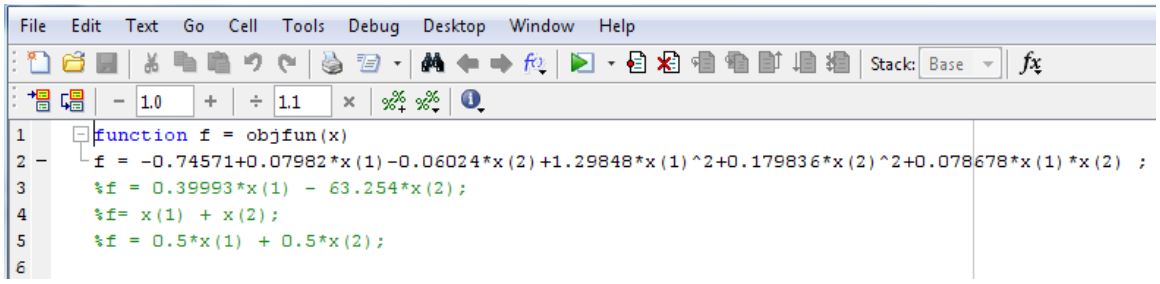

2. Define the constraints

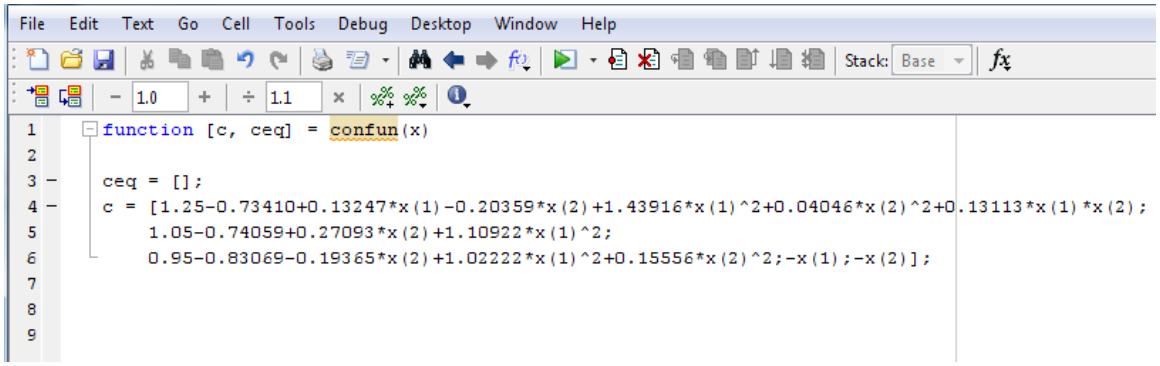

3. Order optimization

```
clear all;
x0 = [-1,1];      % Make a starting guess at the solution
Lb = [-2 -2];
Ub = [2 2];
options = optimset('LargeScale','off');
[x,fval] = ...
fmincon(@objfun,x0,[],[],[],[],Lb,Ub,@confun,options)
%fmincon(f1,x0,[],[],[],[],[],[],@confun,options)
```

4. Graphical contour plot

```
%%%%%%%%%%%%%%%%%%%%%%%%%%%%%%%%%%%%%%%%%%%%%%%%%%%%%%%%%%%%%%%%%%%%%%%%%%%%%%%%%%%%%%%%%%%%%%%%%%%%%%%%%%%%%%%%
% Examples of Contour Plot
%%%%%%%%%%%%%%%%%%%%%%%%%%%%%%%%%%%%%%%%%%%%%%%%%%%%%%%%%%%%%%%%%%%%%%%%%%%%%%%%%%%%%%%%%%%%%%%%%%%%%%%%%%%%%%%%

[ X1, X2 ] = meshgrid( -2 : .1 : 2, -2 : .1 : 2 ) ;
Y = -0.74571 + 0.07982 .* X1 - 0.06024 .* X2 + 1.29848 .* X1 .^ 2 + 0.179836 .* X2 .^ 2 + 0.078678 .* X1 .* X2 ;
Y1 = 1.25 - 0.73410 + 0.13247.*X1 - 0.20359.*X2 + 1.43916.*X1.^2 + 0.04046.*X2.^2 + 0.13113.*X1.*X2;
Y2 = 1.05 - 0.74059 + 0.27093.*X2 + 1.10922*X1.^2;
Y3 = 0.95 - 0.83069 - 0.19365.*X2 + 1.02222.*X1.^2 + 0.15556.*X2.^2;

figure( 1 ) ;
[ C, h ] = contour( X1, X2, Y, 5 ) ;hold on
[ C, h ] = contour( X1, X2, Y1, 20 ) ;
[ C, h ] = contour( X1, X2, Y2, 5 ) ;
[ C, h ] = contour( X1, X2, Y3, 5 ) ;
%set( h, 'ShowText', 'on', 'TextStep', get( h, 'LevelStep' ) * 2 ) ;
colormap cool ;
xlabel( 'Normalized nozzle Angle (X_{1})' ) ;
ylabel( 'Normalized coolant Flow Rate (X_{2})') ;
title('Minimization of normalized wear rate vs nozzle angle,coolant flow rate');
```

AUTHOR BIOGRAPHY

Author	Katchamart Manokruang
Date of Birth	June 8, 1983
Bachelor Degree	B.S. Production Engineering
Institute	Department of Production Engineering Faculty of Engineering King Mongkut's University of Technology North Bangkok
Year of Graduation	2006
Undergraduate Research	Parametric Study of Diamond Wheel Dicing Process Improvement
Scholarship	Graduate Scholarship, Western Digital
Experience	Engineer at Western Digital (From 2006-Currently) 2009 – Currently Robot Sort, SDET Robot Sort, Bar Align and Head Part 2006-2009 Stripe High Grinding and Bar Divided